

# Determination of Active Vitamin D Levels, Synthesis, Demand, and Utilization

Sean Robert Maloney (✉ [SRMaloney1@msn.com](mailto:SRMaloney1@msn.com))

---

## Research

**Keywords:** Vitamin D, Viral Replication, Inflammatory Response, Immune System, COVID-19

**Posted Date:** May 10th, 2022

**DOI:** <https://doi.org/10.21203/rs.3.rs-1637864/v1>

**License:**  This work is licensed under a Creative Commons Attribution 4.0 International License.

[Read Full License](#)

---

Pages: 54, Words 16,931 - 08 May 2022

Figures: 1, 2a, 2b, 2c, 2d

References: 63, Appendices 1

Corresponding Author: Sean R Maloney

Emails: [SRMaloney1@msn.com](mailto:SRMaloney1@msn.com)

[sean.maloney@va.gov](mailto:sean.maloney@va.gov)

Tele: 336-406-6626

Guarantor: Sean R Maloney

## Determination of Active Vitamin D Levels, Synthesis, Demand and Utilization

Sean R. Maloney, M.D., MS Mech. Eng., BS Chem. Eng.\*

Matthew R. Maloney Ph.D.\*\*

\*Department of Rehabilitation Medicine \*

W.G. (Bill) Hefner VA Medical Center

1601 Brenner Avenue

Salisbury, NC 28144

\*\*Quantitative Model Consulting

1428 Clover Lane

Ft. Collins, CO 80521

[maloney.matthew@gmail.com](mailto:maloney.matthew@gmail.com) , (919) 215-4995

**FUNDING:** Salisbury Foundation for Research and Education, National Association of Veterans' Research and Education Foundations, NAVREF

## Abstract/Summary

Measurement of plasma (serum) 25(OH)D<sub>3</sub> levels, (the precursor of active vitamin D) is the current method of evaluating vitamin D status. The measurement of active vitamin D, 1,25(OH)<sub>2</sub>D<sub>3</sub> and its precursor, 25(OH)D<sub>3</sub>, in the serum does not always reflect the overall active vitamin D synthesis and utilization by the body. This may be especially true during periods of increased demand for this hormone. Active vitamin D synthesis and degradation can occur simultaneously and is often entirely an intracellular process. The process whereby much of active vitamin D is synthesized and degraded and how it is transported out of the cell and body is presented. A method of determining active vitamin D levels, synthesis, degradation, and utilization is also presented based on the measurement of the end metabolites of active vitamin D and of its precursor vitamin D.

Unlike other vitamins, active vitamin D is a hormone acting on many receptor sites in the body and it is an essential modulator of the immune system. The vitamin D hormone plays an active role in the initial suppression of invading microbials including viruses and in subduing the body's inflammatory response to acute viral infections and reactivation of latent viruses. The conversion of precursor vitamin D supplements to active vitamin D may be hindered in individuals with elevated body mass Index (BMI) or percent body fat when initial stores of vitamin D precursors are low and demand for active vitamin D increases suddenly such as during acute systemic infections, trauma, or other physiological stressors.

In this paper, a molar balance approach involving vitamin D end metabolites is used to estimate fluctuating active vitamin D levels, synthesis, and demand. The ability to estimate active vitamin D levels, and synthesis may allow the establishment of actual active vitamin D levels in the body needed to suppress COVID-19 virus replication and to decrease COVID-19 virus stimulation of an exaggerated immune system inflammatory response. Determining actual active vitamin D levels and percent utilization/demand may prove vital in the treatment and monitoring of individuals with acute and sometimes life-threatening infections. This new information may allow clinicians to quickly adjust intervention with calcitriol, active vitamin D, 1,25(OH)<sub>2</sub>D<sub>3</sub>, in order to achieve rapid suppression of viruses such as the COVID-19 virus and improvement in immune system's ability to control its inflammatory response.

**KEYWORDS:** Vitamin D, Viral Replication, Inflammatory Response, Immune System, COVID-19

## Introduction

There have been numerous studies recently which have linked increased COVID 19 morbidity and mortality to low vitamin D states.<sup>1-5</sup> Likewise, there have been recent review articles which discuss reasons why low vitamin D states may play a role in a patient's ability to fight off or mitigate the morbidity and mortality associated with a COVID-19 infection.<sup>6-8</sup> Central to this new focus on vitamin D status is the important role that vitamin D plays in the modulation of the immune system.<sup>9-11</sup> Immune system cells with vitamin D receptors exist in large numbers in many tissues of the body including primary lymphoid organs (bone marrow and thymus) and secondary lymphoid organs (lymph nodes, the spleen, the tonsils, skin, and various mucous membrane layers in the body including those of the nose, throat, and bowel).<sup>12</sup> An important recent article reviews the relationship between co-morbidities in Covid-19 patients known to be associated with increased morbidity and mortality and those same co-morbidities in low vitamin D states.<sup>13</sup>

Persistent low vitamin D states may chronically impair the immune system in individuals in two ways. First, in low vitamin D states, the immune system may be unable to maximally suppress viruses such as COVID-19 in part due to inadequate production of cathelicidin and defensin  $\beta 2$ .<sup>14-16</sup> Second, vitamin D is a hormone which acts directly on the immune system including B and T lymphocyte cells to down regulate the inflammatory reaction triggered by viral antigens, or other microorganisms.<sup>17</sup>

Plasma 25(OH)D<sub>3</sub> vitamin D precursor levels represent vitamin D stores in the body and have been traditionally measured to assess vitamin D status. This paper will build on and review evidence supporting the following two premises: 1) plasma 25(OH)D<sub>3</sub> levels do not consistently represent active vitamin D synthesis (levels), demand, or utilization by the body, and 2) the need for and utilization of active vitamin D by tissues of the body can vary between individuals and dramatically in the same individual under different circumstances. Many factors can reduce a person's ability to produce active vitamin D including low vitamin D precursor stores especially associated with increased body mass index, BMI (i.e., obesity), decreased exposure to UVB light, increasing age, exogenous medications, and genetic factors.

The measurement of active vitamin D, 1,25(OH)<sub>2</sub>D<sub>3</sub>, plasma levels is possible and in certain situations is indicated. This paper will present information to support the premise that serum active vitamin D levels often do not correlate with vitamin D precursor levels and may not correlate well with active vitamin D synthesis in the body. This paper uses a molar balance approach to better assess active vitamin D status.

## Description of the Vitamin D Molar Balance Model

A molar balance approach to analyze active vitamin D synthesis and degradation is presented in this paper. Instead of focusing on the front end (input) and back end (output) of the vitamin D synthesis pathway, this paper will focus only on the back end (output) of the vitamin D synthesis pathway. This molar balance approach may permit 1) an estimation, at one point in time (t), of the amount of active vitamin D that has been recently produced in the body, 2) the determination (based on measurable quantities) of the synthesis of active vitamin D,  $1,25(\text{OH})_2\text{D}_3$ , over 24 hours, 3) the evaluation of the body's overall demand for active vitamin D at a given point in time (t) by comparing the amount of active vitamin D precursor,  $25(\text{OH})\text{D}_3$ , used to synthesize active vitamin D to the amount active vitamin D precursor, that is diverted away from the synthesis of active vitamin D and metabolized (wasted). Knowing the demand for active vitamin D, and the percent utilization of active vitamin D precursor to produce active vitamin D, may help to determine whether inadequate, adequate, or excess vitamin D precursor is present. Measurement of the above vitamin D characteristics may enable clinicians to better identify individuals who may have impaired immune system function associated with inadequate active vitamin D synthesis and to better treat these individuals when they have COVID – 19 viral or other acute infection infections. Similarly, measurement of these characteristics may allow clinicians to better treat those individuals with chronic inflammation associated with latent, partially reactivated, latent viruses .

The  $25(\text{OH})\text{D}_3$  molar balance model is depicted qualitatively in Figures 1, and 2a-d, and is described quantitatively in several equations included in this text as well as in a more rigorous manner in Appendix A. The figures and equations included in this text along with Appendix A describe the active vitamin D precursor ( $25(\text{OH})\text{D}_3$ ) transport, conversion to active vitamin D, metabolism and excretion from the body. In this molar balance model, the body is divided into two main compartments for simplicity. The extracellular compartment is made up of all those spaces in the body which are not made up of cells and which contain fluids such as plasma, lymphatic fluid, bile, interstitial fluid etc. The intracellular compartment is the space made up all those cells in the tissues of the body.

For the purpose of this model, the spaces which are made up of urine in the bladder and stool in the distal small bowel and large bowel are considered outside the body since the end metabolites of vitamin D are assumed lost to the intracellular and extracellular spaces of the body once they enter these spaces. The cells of bladder and bowel tissues including the cells of their mucosal linings are in the intracellular space/compartment of the body.

This model also describes the synthesis and transport of active vitamin D,  $1,25(\text{OH})_2\text{D}_3$ , and its inactive metabolites into and out of the intracellular and extracellular compartments of the

body at any arbitrary time(t) and over an arbitrary, 24-hour, interval of time. The relationship between the end inactive metabolites of  $1,25(\text{OH})_2\text{D}_3$  and the end inactive metabolites of  $25(\text{OH})\text{D}_3$  (that are diverted away from  $1,25(\text{OH})_2\text{D}_3$  synthesis i.e., wasted) are used to establish changing active vitamin D demand and changing vitamin D precursor,  $25(\text{OH})\text{D}_3$ , utilization by the body to synthesize active vitamin D.

This model may also provide a better understanding of why: 1) the same store or concentration of  $25(\text{OH})\text{D}_3$  in the plasma may result in different overall (increased or decreased) rates of  $1,25(\text{OH})_2\text{D}_3$  synthesis in cells of the tissues of the body, 2) the same store or concentration of  $25(\text{OH})\text{D}_3$  in the plasma may result in an adequate rate of  $1,25(\text{OH})_2\text{D}_3$  synthesis for one individual but not for another or for one individual experiencing increased active vitamin D demand over their usual vitamin D demand state.<sup>18-20</sup> and 3) a significant portion of  $\text{D}_3$  can be converted from vitamin  $\text{D}_3$  to  $25(\text{OH})\text{D}_3$  and then to  $1,25(\text{OH})_2\text{D}_3$  in the same cell without this portion of the body's vitamin D precursor,  $25(\text{OH})\text{D}_3$ , ever passing through the plasma (sub-extracellular) space before being converted to  $1,25(\text{OH})_2\text{D}_3$ .<sup>21</sup>

The active form of vitamin D is a hormone and is structurally different from its precursor molecules and its inactive metabolites. This difference allows active vitamin D to attach to receptor sites in or on target cells in order to activate different genes and chemical reactions. As a result of a body's changing demand or need for active vitamin D, cells/tissues in the body can produce increasing or decreasing amounts of the active form of vitamin D,  $1,25(\text{OH})_2\text{D}_3$ , from its precursor,  $25(\text{OH})\text{D}_3$ . The source of vitamin D precursor needed for this synthesis can come from vitamin D precursor already present in the body's cells/ tissues, or from vitamin D precursor entering the body's cells/tissues from the plasma space.

In a patient with a low normal serum  $25(\text{OH})\text{D}_3$  level, low normal stores of vitamin D precursors in their body's fat, and elevated BMI, their ability to increase active vitamin D synthesis by consuming increased exogenous vitamin D precursor supplementation ( $\text{D}_3$  or  $25(\text{OH})\text{D}_3$ ) drops as a function of increasing BMI. This occurs because the additional exogenous vitamin D precursors are quickly sequestered into their body's fat tissue (due to the higher concentration of serum precursors in the plasma) and are unavailable to increase the synthesis of active vitamin D in other cells. The relative long half-lives of the vitamin D precursors in the body being converted to active vitamin D further contributes to the diversion of vitamin D precursors from the plasma to fat cells.

For patients with high BMI's and sudden increasing demand for active vitamin D, The only practical way to increase active vitamin D levels to meet increasing demand may be to take over control of active vitamin D levels in the body by supplementing these patients with active vitamin D, calcitriol, until demand for active vitamin D decreases or until concentration of

active vitamin D precursors increase in fat tissues to support high enough levels of vitamin D precursors in the plasma to support increased demand for active vitamin D.

The body's ability to increase the intracellular synthesis of active vitamin D is limited by the amount of vitamin D precursor stored in the body (including plasma). The changing need for active vitamin D can occur in cells/tissues which cannot completely synthesize their own active form of vitamin D but rely on plasma vitamin D precursor, 25(OH)D<sub>3</sub>, or rely on active vitamin D, 1,25(OH)<sub>2</sub>D<sub>3</sub> from other cells/tissues of the body (endocrine source). There are also the cells/tissues that can synthesize their own active vitamin D (autocrine or paracrine source for active vitamin D). Some cells/tissues that store vitamin D precursors, can produce their own active vitamin D independently of the extracellular plasma source of the vitamin D precursor, 25(OH)D<sub>3</sub>.

Changing demand and synthesis of active vitamin D has been documented in several studies. One recent study which compared active vitamin D serum levels in non-pregnant women with those in pregnant women found significantly increased active vitamin D levels in those who were pregnant. Mean levels of active vitamin D, 1,25(OH)<sub>2</sub>D<sub>3</sub>, at 15 weeks were as follows: non-pregnant controls, 85.6 pmoles/L, non-preeclamptic pregnant women, 336.3 pmoles/L, and preeclamptic pregnant women 388.8 pmoles/L.<sup>22</sup> Mean serum 25(OH)D<sub>3</sub> levels in the same groups respectively were 46.8 nmoles/L, 44.7 nmoles/L, and 33.1 nmoles/L. In the first two groups of women, mean serum 25(OH)D<sub>3</sub> levels were similar, but mean serum 1,25(OH)<sub>2</sub>D<sub>3</sub> levels varied by a factor of 4.

In comparing the mean serum 25(OH)D<sub>3</sub> levels of the last two groups of pregnant women, the pre-eclamptic women had a lower mean serum 25(OH)D<sub>3</sub> level but a higher mean serum 1,25(OH)<sub>2</sub>D<sub>3</sub> level. These findings represent a dramatic example of uncoupling of mean serum 25(OH)D<sub>3</sub> and 1,25(OH)<sub>2</sub>D<sub>3</sub> levels when comparing non-pregnant and pregnant women's levels and to a lesser extent when comparing pregnant and pre-eclamptic pregnant women's levels.

An increase in vitamin D utilization/demand has been documented by serial measurements of dropping serum vitamin D precursor, 25(OH)D<sub>3</sub> levels during military training over a short duration.<sup>23</sup> During a 1993 study of nutritional status in young healthy US Army soldiers undergoing an arduous 21 day Special Forces Evaluation and Selection Program, serum vitamin D precursor, 25(OH)D<sub>3</sub> levels dropped from an initial mean level of 61ng/ml (range 34-100 ng/ml) on the first day to a mean level of 55 ng/ml (range 38-97 ng/ml) on day 10, to a mean level of 51 ng/ml (range 42-60) by day 20. The statistical significance of this drop was not tested at the time perhaps in part because vitamin D was only one of many nutritional status biomarkers that were measured and because mean vitamin D levels remained above the upper limits of normal (50 ng/ml at the time). To approximately convert ng/ml to nmoles/L, multiply ng/ml by 2.5.

Vitamin D binding protein and total and free vitamin D metabolites have been shown to have a changing or diurnal rhythm (i.e. repeated daily pattern of change in vitamin D metabolite levels during the day).<sup>24</sup> A recent case study of a middle-aged woman, who was taking 5000 IU's of vitamin D<sub>3</sub> orally each afternoon for over one year, demonstrated not only a daily serum 25(OH)D<sub>3</sub> diurnal rhythm but also a temporary significant drop in serum 25(OH)D<sub>3</sub> level associated with an acute but short duration respiratory illness.<sup>25</sup> The study included four separate days of evaluation, 10/11, 10/18, 11/15, and 11/28/2017) and the midday serum 24(OH)D<sub>3</sub> levels on each of these days was: 67 ng/ml, 65 ng/ml, 51 ng/ml (at the time of a brief cold) , and 67 ng/ml, respectively. The approximate drop of 25% on day three was significant, P < 0.013.

The level of vitamin D precursor, 25(OH)D<sub>3</sub>, in the plasma is often not proportional to the level of active vitamin D, 1,25(OH)<sub>2</sub>D<sub>3</sub> in the plasma and does not directly indicate a rate of active vitamin D synthesis. This occurs in part because a significant portion of active vitamin D can be synthesized and metabolized in cells/tissues of the body without active vitamin D precursor, 25(OH)D<sub>3</sub>, or active vitamin D ever passing through the plasma space. This observation is supported by the concurrent presence of the enzymes that allow the conversion of D<sub>3</sub> to 25(OH)D<sub>3</sub> and the enzyme that allows the conversion of precursor 25(OH)D<sub>3</sub> to active vitamin D, 1,25(OH)<sub>2</sub>D<sub>3</sub>, in some cells/tissues of the body. The enzymes (CYP2R1, CYP3A4, and CYP27A1) which convert D<sub>3</sub> to 25(OH)D<sub>3</sub>, the enzyme (CYP27B1) which converts 25(OH)D<sub>3</sub> to 1,25(OH)<sub>2</sub>D<sub>3</sub>, and the enzyme (CYP24A1) which converts 25(OH)D<sub>3</sub> and 1,25(OH)<sub>2</sub>D<sub>3</sub> to inactive forms of vitamin D (i.e., 24,25(OH)<sub>2</sub>D<sub>3</sub>, 23,25(OH)<sub>2</sub>, 1,24,25(OH)<sub>3</sub>D<sub>3</sub> and 1,23,25(OH)<sub>3</sub>D<sub>3</sub>) are described in more detail in other publications.<sup>26-27</sup>

The RNA expression of these enzymes has been examined recently in 27 different tissues of 95 human subjects as part of a larger study of gene expression.<sup>28</sup> The units of gene transcript expression are RPKM (i.e., Reads per Kilobase of transcript, per Million mapped reads).<sup>29</sup> In comparing/interpreting the RPKM reads, (i.e. comparing the ability of cells/tissues to produce vitamin D and its metabolites), it is important to note that RPKM reads represent the density of RNA in the tissue sample and not the overall size of the tissue or organ. Thus, the ability of tissues and organs to produce enzymes or process substrate will also depend on the total relative size of the tissue or organ and other factors such as the rate of diffusion or perfusion of the substrates through the tissue. The following four paragraphs outline the presence of the enzymes of vitamin D metabolism in many of the cells/tissues of the body.

The CYP27A1 enzyme had the greatest representation in the body among the three enzymes which convert D<sub>3</sub> to 25(OH)D<sub>3</sub>.<sup>30</sup> Of the 27 tissues studied, liver was the tissue with the highest expression of this gene (approx. 101.4 RPKM), followed by small intestine (27.6 RPKM), lung (approx. 26 RPKM), and duodenum ( approx. 23 RPKM). However, most of the other tissues examined had significant expression of this enzyme RNA including prostate (18 RPKM), kidney

(18 RPKM), adrenal (12 RPKM), ovary (11 RPKM), brain-colon-urinary bladder (9 RPKM), lymph node tissue (8 RPKM) and fat (6 RPKM). The second most widely distributed enzyme RNA (but of lower concentration) for this first conversion,  $D_3$  to  $25(OH)D_3$ , was CYP2R1.<sup>31</sup> This enzyme was most highly expressed in skin (2.2 RPKM). Other tissue representation included testes (2.0 RPKM), duodenum (approx. 1.27 RPKM), small intestine (1.25 RPKM), appendix (1.36 RPKM), lymph node tissue (1.1 RPKM), spleen (1.0 RPKM), fat & thyroid (0.9 RPKM) and bone marrow (0.45 RPKM). The third enzyme for the conversion of  $D_3$  to the vitamin  $D_3$  precursor,  $25(OH)D_3$  was CYP3A4.<sup>32</sup> This enzyme was largely expressed in only three tissues: liver (476.5 RPKM), small intestine (282.8 RPKM), and duodenum (approx. 250 RPKM).

Enzyme CYP27B1 converts  $25(OH)D_3$  to the active form of vitamin D,  $1,25(OH)_2D_3$ .<sup>33</sup> Its RNA was present in almost all of the tissues studied but most significantly present in kidney (9.5 RPKM) and thyroid (4.8 RPKM), followed by appendix (approx. 0.9 RPKM), lymph node (0.8 RPKM), bone marrow & adrenal tissue (0.4 RPKM), and fat (0.1 RPKM).

CYP24A1 is the enzyme which metabolizes both  $25(OH)D_3$  and  $1,25(OH)_2D_3$  to the inactive forms  $24,25(OH)_2D_3$ ,  $23,25(OH)_2D_3$ ,  $1,24,25(OH)_3D_3$ , and  $1,23,25(OH)_3$  respectively as well as to their end metabolites.<sup>27,34</sup> The catabolic CYP24A1 enzyme RNA is present in many tissues, and is highly present in urinary bladder (approx. 21.5 RPKM), and endometrium (10.7 RPKM), followed by kidney (approx. 3.5 RPKM), and placenta (approx. 2.5 RPKM). The high levels of CYP24A1 enzyme in the endometrium and placenta may be required due to the increased  $1,25(OH)_2D_3$  synthesis during pregnancy.

The RNA expression study from which the above data is taken<sup>28</sup> did not include skeletal muscle tissue, and it is not known if enzyme RNA for both steps in the conversion of  $D_3$  to  $1,25(OH)_2D_3$  exist in skeletal muscle. However, CYP27B1 has been found to be present in skeletal muscle.<sup>35-37</sup> In this molar balance analysis,  $D_2$  and its metabolites, and C-3-epi- $25(OH)D_3$  and  $1,25(OH)_2$ -3-Epi- $D_3$  are ignored to simplify the model.<sup>38</sup>

The concurrent existence of DNA genes and their resulting RNA that code for enzymes capable of converting  $D_3$  to  $25(OH)D_3$  (3 possible enzymes) and  $25(OH)D_3$  to  $1,25(OH)_2D_3$  (1 enzyme) in many different tissue locations suggests the existence of a synthesis pathway from  $D_3$  to  $1,25(OH)_2D_3$  in cell/tissue types that are independent of the need for transported extracellular (plasma) compartment  $25(OH)D_3$  generated from the liver. The presence of RNA for a particular enzyme does not necessarily equate to a functional protein being translated from the RNA and the functionality of the proteins would need to be verified. The large presence of immune system cells in many tissues of the body makes the immune system potentially one of the largest producers and consumers of active vitamin D during certain conditions such as severe infections especially involving multiple tissues such as with COVID – 19 virus infections.

An alternate, strictly intracellular,  $1,25(\text{OH})_2\text{D}_3$  synthesis and degradation pathway supports the idea that extracellular (plasma) compartment  $25(\text{OH})\text{D}_3$  and  $1,25(\text{OH})_2\text{D}_3$  levels are partially uncoupled from intracellular compartment active vitamin D synthesis. An intracellular active vitamin D synthesis pathway independent of plasma,  $25(\text{OH})\text{D}_3$ , may explain why the rate of active vitamin D,  $1,25(\text{OH})_2\text{D}_3$ , synthesis is partially independent from the aqueous (plasma) vitamin D precursor,  $25(\text{OH})\text{D}_3$  concentration. Figure 1 provides a diagrammatic picture of the movement of vitamin D through the body and between the intracellular and extracellular compartments of the body. The blue arrow in Figure 1 depicts an intracellular synthesis pathway for  $1,25(\text{OH})_2\text{D}_3$  without its precursor  $25(\text{OH})\text{D}_3$  ever having to pass through or to be initially stored in the extracellular plasma space.

Serum  $25(\text{OH})\text{D}_3$  levels and  $1,25(\text{OH})_2\text{D}_3$  levels do not appear to have a proportional relationship, and serum  $25(\text{OH})\text{D}_3$  concentration in the plasma space may not necessarily reflect the body's ability to meet the need for active vitamin D synthesis. The following mathematical equations for the molar balance analysis are based on and depend on the accurate measurement of changing concentrations of vitamin D end metabolites in plasma and urine samples. This model can be used to estimate active vitamin D synthesis and to assess whether the body's demand for vitamin D is being met. Again, this molar balance method of assessing vitamin D status analyzes and depends primarily on the backend of the vitamin D metabolic pathway rather than the frontend.

Some data concerning where vitamin  $\text{D}_3$  and  $25(\text{OH})\text{D}_3$  are stored in the body exists based on intravenous radiolabeled vitamin D studies.  $\text{D}_3$  has been shown to accumulate the most in adipose tissue but  $\text{D}_3$  also accumulates in muscle, skin, plasma, and other organs. Total body storage of vitamin precursors has been estimated to be approximately 1 micro-mole ( $10^{-6}$  moles) with two-thirds stored as  $\text{D}_3$  (primarily in adipose tissue) and the rest primarily stored as  $25(\text{OH})\text{D}_3$  in various tissues and fluids including adipose tissue 35%, muscle 20%, and plasma/extracellular fluid 30%.<sup>39,40</sup> The molar balance model divides the storage of vitamin D into two compartments: intracellular and extracellular. Plasma is considered a sub-space of the extracellular compartment. The concentrations of  $25(\text{OH})\text{D}_3$ ,  $1,25(\text{OH})_2\text{D}_3$  and their end metabolites are assumed to be approximately uniform or homogeneous in both the plasma and total extracellular spaces. In contrast, levels of vitamin D precursors and active vitamin D are not assumed to be homogeneous within the cells/tissues of the intracellular compartment or spaces.

Using radioactive H<sup>3</sup> tagging, attempts have been made in several studies to determine the portion of vitamin D and its metabolites excreted in the urine versus in the stool (through bile).<sup>41-43</sup> In three studies approximate differences between excretion in the urine versus in the stool have been as follows: 32% versus 68% <sup>41</sup> (n = 7), 25% versus 75% <sup>42</sup> (n = 7), and 22% versus 78% <sup>43</sup> (n = 16). The molar balance model uses the values of 25% excretion in the urine and 75% in the stool.

## **Model Assumptions:**

### **1) Assumption: Constant Compartment Volumes**

The volume of the body's extracellular compartment or space,  $V_e$ , (or plasma sub-compartment,  $V_p$ ) can change in certain circumstances such as pregnancy, severe dehydration or congestive heart failure. However, for our model, it is assumed that the extracellular (or plasma) volumes at some initial time,  $t_0$ ,  $V_e(t_0)$ , equals the extracellular compartment volume at some later time,  $t_1$ ,  $V_e(t_1)$ , and equals a constant  $V_e$ . Similarly, the body's intracellular volume,  $V_i$  is assumed to be constant.<sup>44,45</sup> See figure 2c. notes.

### **2) Assumption: Intracellular volume = 2x Extracellular Volume**

For a complete list of different volume assumptions for men and women see Figure 2c note, "Intracellular and Extracellular Compartment Volume Analysis".

### **3) Assumption: The $C_n$ Intracellular Concentration of end metabolites = $\beta$ x The $C_n$ Extracellular Concentration**

The mean intracellular concentrations of the end metabolites,  $m_n$ , will be assumed to be proportional to and a factor  $\beta$  times the same concentrations in the extracellular compartment. The  $\beta$  factor is greater than 1 in this model because the end metabolites are assumed to be transported from the intracellular compartment (where they are made) to the extracellular compartment by a concentration gradient in order to be excreted from the body. (See Figure 2d.)

#### **4) Assumption: Extracellular Sub-compartment $C_n$ Concentrations are Equal.**

Vitamin D metabolite,  $m_n$ , concentrations may differ somewhat between extracellular sub-compartments/spaces and their concentration gradients around cells may vary. However, in our model, the concentrations of  $25(\text{OH})\text{D}_3$  and its many metabolites (including  $1,25(\text{OH})_2\text{D}_3$ ) are assumed to be uniform for the same metabolites across different extracellular sub-compartments at any given point in time.

#### **5) Assumption: NMOLES of Active Vitamin D Synthesized over 24 hours Equals the NMOLES of Active Vitamin D End Metabolites Synthesized over the Same 24 hrs.**

The Molar Balance Model for active vitamin D synthesis assumes that the number of nmoles of active vitamin D synthesized over a 24-hour period equals the sum of the number of nmoles of end metabolites of active vitamin D synthesized over the same 24 hours. This steady state assumption, further depends on the following: 1) any change in the total body's number of nmoles of active vitamin D or in the number of nmoles of active vitamin D intermediate metabolites in the intracellular plus extracellular compartments is small compared to the synthesis of active vitamin D end metabolites over 24 hours, and 2) the number of nmoles of active vitamin D and active vitamin D intermediate metabolites excreted is relatively small compared to the nmoles of end metabolites excreted over the same 24 hour period. All the measurements made using this and the following assumptions are in units of nmoles. The fact that this measurement is made over 24 hours allows this measurement also to represent active vitamin D synthesis per 24 hours (a synthesis rate).

The equations derived to determine the nmoles of active vitamin D synthesized over 24 hours depend on the above assumptions. The validity of these assumptions could be checked by doing second serum and urine assays which measures total end metabolites of active vitamin D precursor, active vitamin D, and all of their intermediate metabolites after all active vitamin D precursor, active vitamin D, and its intermediate metabolites are driven to their end metabolites by adding significant excess CYP24A1 hydroxylase enzyme. If, after adding measured nmoles of serum active vitamin D and its precursor,  $25(\text{OH})\text{D}_3$ , to the measurement of their end metabolites in the first sample, a discrepancy between the sum of these metabolites in the first sample and the total end metabolites of  $25(\text{OH})\text{D}_3$  and  $1,25(\text{OH})_2\text{D}_3$  in the second sample exists, then a correction factor can be added to the calculation. (See further discussions below and in Appendix A.)

**6) Assumption: NMOLES of End Metabolites,  $m_{8:10}$ , in the Intracellular Plus Extracellular Spaces Can Be Used to Estimate the NMOLES of Active Vitamin D Synthesis (Levels) at Time (t).**

The total nmoles of active vitamin D,  $1,25(\text{OH})_2\text{D}_3$  end metabolites ( $m_8$ ,  $m_9$ , and  $m_{10}$ ) in the extracellular plus intracellular spaces, can be used to estimate the body's total active vitamin D synthesis at any point in time, (t). The assumption in the sentence above allows for a quicker method for assessing active vitamin D synthesis at any given time (t) from a single plasma sample and to track changes in active vitamin D synthesis due to exogenous vitamin D supplementation. The use of only the end metabolites of active vitamin D as a biomarker for active vitamin D synthesis only approximates active vitamin D synthesis when the levels (synthesis) of active vitamin D and its intermediate metabolites are changing significantly (going up or down) as the demand and synthesis of active vitamin D changes.

As with the 24-hour assessment above, a second plasma serum assay could be performed which measures the total end metabolites of active vitamin D after all active vitamin D and its intermediate metabolites are driven to their end metabolites by the CYP24A1 hydroxylase enzyme. This assay could be used to check for a significant buildup of active vitamin D intermediate metabolites relative to active vitamin D end metabolites. If the discrepancy is large then a factor to correct for this discrepancy must be added to the molar balance model calculation. This same analysis could be performed on a spot urine although the dilution variability of spot urines would have to be accounted for. (See Figures 2a and 2b and assumptions A.7 and A.8 and their description in Appendix A on pages 38-39.)

**7) Assumption: The total end metabolites of  $25(\text{OH})\text{D}_3$  in the extracellular and intracellular spaces that are not metabolized from  $1,25(\text{OH})_2\text{D}_3$  represent the nmoles of vitamin D precursor,  $25(\text{OH})$ , that are diverted away from the synthesis of active vitamin D at any point in time (t).**

Determination of the total nmoles of  $m_6$  and  $m_7$  (end metabolites of  $m_0$ ) in the extracellular and intracellular spaces at time (t) are assumed to represent the total number of nmoles of  $25(\text{OH})\text{D}_3$  diverted away from the synthesis of active vitamin D at time (t). This assumption further assumes that the nmoles of diverted  $25(\text{OH})\text{D}_3$  ( $m_0$ ) intermediate metabolites are small in number compared to the end metabolites of diverted  $25(\text{OH})\text{D}_3$  ( $m_0$ ). The assumption in the sentence above allows for a quicker method 1) to assess the total nmoles of vitamin D precursor,  $25(\text{OH})\text{D}_3$  diverted away from the synthesis of active vitamin D at any given time (t) from a single plasma sample and 2) to track changes in active vitamin D precursor diversion following exogenous vitamin D supplementation.

The validity of this assumption can be checked by doing a second serum assay from a plasma sample drawn at time (t) which measures total end metabolites of active vitamin D precursor,  $m_0$ , after 25(OH) vitamin D and all active vitamin D precursor intermediate metabolites are driven to their end metabolites by CYP24A1 hydroxylase enzyme. In this case, the number of nmoles of active vitamin D precursor,  $m_0$ , originally in the serum level of the plasma sample must be subtracted from the measured diverted end metabolites of  $m_0$ . The diverted nmoles of active vitamin D are used in the calculation of the active vitamin D demand ratio and in the determination of the percent utilization of active vitamin D precursor,  $m_0$ , in the synthesis of active vitamin D.

**8) Assumption: This model assumes that 25% of 1,25(OH)<sub>2</sub>D<sub>3</sub> and its metabolites are excreted in the urine and 75% are excreted in the stool from bile. (See text below)**

## Model Derivation through Figures and Equations

Based on the above assumptions, Figures 2a -2d in this paper and the following equations in this paper (including in appendix A), the synthesis of and demand for active vitamin D, 1,25(OH)<sub>2</sub>D<sub>3</sub> by the many cells/tissues of the body is estimated, and the percent utilization of vitamin D<sub>3</sub> precursor, 25(OH)D for the synthesis of active vitamin D by the body is determined.

Finding a way to estimate the nmoles of intracellular 1,25(OH)<sub>2</sub>D<sub>3</sub> synthesized in the body at any point in time (t) or over a period of time ( $t_1 - t_0$ ) such as 24 hours (in nmoles) could be used to identify changing demand for active vitamin D. Determination of the change in total end inactive metabolites of 1,25(OH)<sub>2</sub>D<sub>3</sub> in the extracellular and intracellular compartments of the body over 24 hours (in nmoles), plus the number of nmoles of 1,25(OH)<sub>2</sub>D<sub>3</sub> end inactive metabolites excreted over the same 24 hour period, provides a way to estimate the 24 hour synthesis of intracellular 1,25(OH)<sub>2</sub>D<sub>3</sub>.

Measurement of the nmoles of the end inactive metabolites of 1,25(OH)<sub>2</sub>D<sub>3</sub> excreted from the body in bile/stool during a 24-hour period would be difficult. However, an estimate can be made by measuring the end inactive metabolites in a 24-hour urine sample and then correcting for the number of inactive metabolites excreted by the stool. Based on previous studies,<sup>39-41</sup> this model uses the estimation that 25% of 1,25(OH)<sub>2</sub>D<sub>3</sub> end metabolites are excreted in the urine and 75% are excreted in the stool from bile.

Measuring the nmoles of all of the intermediate and end metabolites of 1,25(OH)<sub>2</sub>D<sub>3</sub> in a plasma specimen or in a 24-hour urine collection would be tedious. However, measurement of

the nmoles of the three primary end metabolites of  $1,25(\text{OH})_2\text{D}_3$  (i.e. 1-OH-23-COOH-24,25,26,27 Tetranor  $\text{D}_3$  or calcitric acid,  $1,25\text{R}(\text{OH})_2\text{D}_3$ -26,23S-lactone or calcitriol-26,23-lactone, and 23-COOH-24,25,26,27 Tetranor  $\text{D}_3$  or Calcioic acid) in a plasma specimen and in a 24 hour urine may allow the approximate determination of active vitamin D,  $1,25(\text{OH})_2\text{D}_3$ , synthesis. This approximation might be achieved by utilizing the 25% excretion in the urine assumption and the other assumptions listed above (See also Appendix A).

Since only 25% of the actual excretion of these three vitamin D end metabolites from the body occurs through the urine, the total excretion of end inactive vitamin D metabolites from the body during the 24-hour period is 4 times the excretion in urine. A finding of different excretion quantities of  $1,25(\text{OH})_2\text{D}_3$  end metabolites over 24 hours occurring at the same plasma  $25(\text{OH})\text{D}_3$  concentration in the same individual under different situations would support one of the assumptions of this model. Namely, the excretion of fluctuating inactive end metabolites of active vitamin D (and by inference fluctuating active vitamin D synthesis) in the body exists which is partially independent of extracellular plasma active vitamin D precursor  $25(\text{OH})\text{D}_3$  levels.

The small letter m and its subscripts n (0-10) are used to identify specific metabolites in the vitamin D synthesis pathway. Figures 2a and 2b describe the enzyme pathways that metabolize  $25(\text{OH})\text{D}_3$ ,  $m_0$ , into the production of active vitamin D hormone,  $1,25(\text{OH})_2\text{D}_3$ ,  $m_1$ , and its metabolites. The enzyme pathways that metabolize  $m_0$  away from the synthesis of active vitamin D into inactive metabolites are part of the body's regulation of the synthesis of active vitamin D and are also described in figures 2a and 2b (see yellow oval).

Figure 2a diagrams some of the intracellular compartment's enzymatic reactions which result in the accumulation of initial and end metabolites of  $25(\text{OH})\text{D}_3$  over some arbitrary time interval ( $t_1 - t_0$ ) in nmoles. Figure 2b. diagrams the rate of synthesis in the intracellular compartment of initial and end metabolites of  $25(\text{OH})\text{D}_3$ ,  $S_{0,n}$ , in units of nmoles/t. Figure 2c presents a simplified diagram of the synthesis, transport of vitamin D metabolites between the intracellular and extracellular compartments, and excretion of vitamin D precursor, active vitamin D, and their end metabolites. Shown with figure 2c are previously measured extracellular, plasma, and intracellular compartment volumes for an average male and female.

Unlike Figure 1 which describes both the front and back ends of the vitamin D metabolic pathways, Figure 2c and 2d describes the back end of the vitamin D metabolic pathways. Figure 2d presents a simpler diagram of the synthesis of the end metabolites of  $25(\text{OH})\text{D}_3$  and  $1,25(\text{OH})_2\text{D}_3$  which are produced in some cells/tissues of the body which contain the CYP24A1 enzyme. This enzyme controls the breakdown of active vitamin D,  $1,25(\text{OH})_2\text{D}_3$  and the portion of active vitamin D precursor,  $25(\text{OH})\text{D}_3$ , which is diverted away from the synthesis of active vitamin D. (See figures 2a and 2b.) The cells/tissues in diagram, 2d, which have unidirectional

arrows represent the cells/tissues that have the enzyme CYP24A1. The cells/tissues in figure 2d which have bidirectional arrows represent the cells/tissues which do not have this enzyme and whose concentrations of these end metabolites may increase or decrease due to passive diffusion of the metabolites from the extracellular compartment.

The pathways from the active vitamin D precursor,  $25(\text{OH})\text{D}_3$ , allow the body to match the synthesis of active vitamin  $\text{D}_3$  to the body's demand for active vitamin  $\text{D}_3$ . If sufficient or more than sufficient vitamin D precursor exists to meet the body's demand for active vitamin D, then the excess can be diverted away from the synthesis of active vitamin D. In figure 2d, the red + signs represent the end inactive metabolites of active vitamin D,  $1,25(\text{OH})_2\text{D}_3$ , or  $m_1$  and the blue + signs represent the end inactive metabolites of the vitamin D precursor,  $25(\text{OH})\text{D}_3$ , or  $m_0$  that are diverted away from the synthesis of active vitamin D. The arrows in Figure 2d represent the flow of metabolites into and out of the intracellular compartment (cells/tissues) and from the extracellular compartment out of the body. The unidirectional arrows represent the flow that is consistently from higher concentrations to lower concentrations. The bidirectional arrows represent gradient dependent, passive flows of metabolites into and out of cells/tissues which are not synthesizing significant quantities of inactive end metabolites of  $25(\text{OH})\text{D}_3$   $m_0$ .

Concepts developed in Figures 2a to 2d are used to develop formulas to estimate the amount of active vitamin synthesized by the body through measurement of the total end metabolites of  $1,25(\text{OH})_2\text{D}_3$  (Integral of  $S_{0,1}$  Eq. 9 & 10 below) produced by cells/tissues of the body over a time interval ( $t_1 - t_0$ ) or to estimate the amount of active vitamin D that has been synthesized in the body at any time ( $t$ ). See appendix A, equations 9,10, and 13, pages 45 - 46. One formula uses the integral of the rate of active vitamin D synthesis, ( $S_{0,1}$ ) over an arbitrary 24-hour time interval to estimate the total synthesis of  $1,25(\text{OH})_2\text{D}_3$  over 24 hours. This synthesis estimate is accomplished by summing the change in the total amount of the end metabolites of  $1,25(\text{OH})_2\text{D}_3$  in the extracellular and intracellular compartments and the accumulation of end metabolites of  $1,25(\text{OH})_2\text{D}_3$  in urine and stool over 24 hours.

So far, this method has focused on the use of the end metabolites of active vitamin D and the end metabolites of its precursor,  $25(\text{OH})\text{D}_3$  (which are formed from vitamin D precursor which is diverted away from the synthesis of active vitamin D) in order to evaluate the actual amount of and the need for active vitamin D synthesis. There is one other consideration concerning the synthesis of active vitamin D and the serum concentration of active vitamin D precursor. Gene CYP27B1 of enzyme C1 Hydroxylase is responsible for the synthesis of active vitamin D from its precursor. (See Figure 2a and the yellow oval, Figure 2b.) and the gene CYP2R1 is responsible for the synthesis of active vitamin D precursor,  $25(\text{OH})\text{D}_3$ , from  $\text{D}_3$ . When these genes become mutated and are no longer able to produce functioning 1- $\alpha$  Hydroxylase or 25-hydroxylase enzymes respectively, severe active vitamin D deficiency can occur.<sup>46</sup>

There may be some genetically variable forms of these deficiencies which may impair the production of their hydroxylase enzymes and effect the production of active vitamin D or its precursor without totally stopping the production of these forms of vitamin D. Measurement of the end metabolites of active vitamin D, of its precursor, 25(OH)D<sub>3</sub>, and of the end metabolites of diverted active vitamin D precursor, may help to determine whether either of these two genes and the production rate of their enzymes may be altered.

A second formula has been derived to determine M<sub>1</sub>(t) (Eq. 13 below) or the amount of end metabolites of active vitamin D, m<sub>1</sub>, that are present in the body at any point in time (t). The amount of end metabolites of active vitamin D in the body at time (t) is then assumed to represent or to be proportional to the amount of active vitamin D synthesized at that moment. The following equations are taken from derivation of equations in Appendix A that quantify active vitamin D synthesis and demand as well as the percent utilization of the precursor to active vitamin D for active vitamin D synthesis.

$$\int_{t_0}^{t_1} S_{0,1}(t)dt = 4.66V_p[(2\beta) + 1] \times [C_{8,p}(t_0, t_1) + C_{9,p}(t_0, t_1) + C_{10,p}(t_0, t_1)] + 4[C_{8:10,u}(t_1)V_u(t_1)] \quad \text{Eq.9}$$

for men where V<sub>p</sub> = 3.0L, V<sub>u</sub>(t<sub>0</sub>) = 0, and β is initially set at 1.1 (App. A)

$$\int_{t_0}^{t_1} S_{0,1}(t)dt = 4.4V_p [(2\beta) + 1] \times [C_{8:10,cp}(t_1, t_0)] + 4[C_{8:10,u}(t_1)V_u(t_1)] \quad \text{Eq.10}$$

for women where V<sub>p</sub> = 2.5L, V<sub>u</sub>(t<sub>0</sub>) = 0, and β is initially set at 1.1

and

$$M_1(t) = M_{8:10}(t) = \beta C_{8:10,cp}(t)2V_e + C_{8:10,cp}(t)V_e \quad \text{Eq.13}$$

where V<sub>e</sub> = 4.66V<sub>p</sub> for men and 4.4V<sub>p</sub> for women and β is set at 1.1

In Appendix A, formulas for a 1,25(OH)<sub>2</sub>D<sub>3</sub> demand ratio,  $\text{Drm}_{1,i+e}(t)$ , Eq.15 below and a 1,25(OH)<sub>2</sub>D<sub>3</sub> 24hrUrine demand ratio,  $\text{Drm}_{1,u}(t_0,t_1)$ , Eq. 16 below are also derived. The rationale for using the ratio of the end inactive metabolites of 1,25(OH)<sub>2</sub>D<sub>3</sub>,  $m_1$ , as the numerator and the end inactive metabolites of 25(OH)D<sub>3</sub>,  $m_0$ , as the denominator is that this ratio will decrease if excess 25(OH)D<sub>3</sub> exists and is shunted away from the synthesis of active vitamin D when the body's active vitamin D supply is adequate and visa versa. Knowing this ratio may be helpful clinically to judge whether there is sufficient vitamin D precursor to meet the needs of the body for active vitamin D synthesis. This concept has been introduced previously based on calculating a calcitriol/calcifediol ratio using this ratio as an indicator of vitamin D hydroxylation efficiency<sup>47</sup> and based on relative vitamin D CYP enzyme activities rather than molar substrate 1,25(OH)<sub>2</sub>D<sub>3</sub> / 25(OH)D<sub>3</sub> ratios.<sup>48</sup> (see pg. 641, figure 37.3 in ref. 45).

$$\text{Drm}_{1,i+e}(t) = \frac{M_{8:10,i+e}(t)}{M_{6:7,i+e}(t)} \quad (\text{Eq.15})$$

$$\text{Drm}_{1,u}(t) = \frac{M_{8:10,u}(t)}{M_{6:7,u}(t)} \quad (\text{Eq.16})$$

An increase in  $m_1$  demand should result in an increase in  $m_1$  synthesis from  $m_0$  accompanied by a decrease in diversion of  $m_0$  away from  $m_1$  synthesis. (i.e. an increase in the  $m_1$  demand ratio) This pattern is suggested in the results of a recent study comparing serum vitamin D metabolites between non pregnant women (controls) and pregnant women (at 15 weeks). One group of pregnant women were without the complication of preeclampsia and one group of pregnant women (at 15 weeks) who went on to develop preclampsia.<sup>22</sup> As stated above, demand for active vitamin D increases during pregnancy. Mean serum active vitamin D levels,  $m_1$ , in these three groups above were respectively: 85.6, 336.3, and 388.8 pmoles/L. The levels of initial inactive 24,25(OH)<sub>2</sub>D<sub>3</sub>,  $m_2$ , metabolites of  $m_0$ , changed in the opposite direction from active vitamin D synthesis and were respectively: 9.7, 6.5, and 3.2 nmoles/L These metabolites decreased in parallel with higher  $m_1$  levels. The differences were not statistically significant but the numbers of subjects were small respectively n: 9, 25, and 25.

A somewhat different pattern was seen in urine samples of one of the initial metabolites of active vitamin D precursor,  $m_0$  which was diverted away from the synthesis of active vitamin D. Mean metabolite  $m_2$ , 24,25(OH)<sub>2</sub>D<sub>3</sub>, levels in the urine of these three groups were respectively :

55.4, 84.1, and 35.6 nmoles/liter.<sup>22</sup> The mean  $m_2$  concentrations in the urine samples decreased in the preeclampsia pregnant group compared to the non-preeclampsia pregnant group suggesting higher utilization % in the pre-eclampsia group. The difference between the  $m_2$  levels between the two pregnant groups was statistically significant. Of note, the other initial intermediate metabolite of  $m_0$ , 23,25(OH) $D_3$  or  $m_3$  which also diverts  $m_0$  away from the synthesis of active vitamin D was not measurable in the urine samples of this study.

A second method for estimating active vitamin D demand would be determination of the % of vitamin D precursor, 25(OH) $D_3$ ,  $m_0$ , that is used to synthesize active vitamin D, 1,25(OH) $_2D_3$ ,  $m_1$ , at one point in time (t) or over 24 hours. The first % utilization measurement,  $Ut_{\%m_{0,i+e}}(t)$ , is presented in Eq. 17 and represents the percent of  $m_0$  utilized at a single point in time (t) based on the measurements of the end metabolites,  $m_{8:10}$  and  $m_{6:7}$  in the intracellular and extracellular compartments. The second measurement of  $m_0$  percent utilization presented in Eq. 18 is based on the measurement of the change in  $m_{8:10}$  and  $m_{6:7}$  end metabolites in the intracellular and extracellular compartments over 24 hours plus the total amount of  $m_{8:10}$  and  $m_{6:7}$  end metabolites excreted in the same 24 hours. (Recall the total body excretion of end metabolites is equal to 4x the amount of end metabolites excreted in urine. See appendix A, page 37-38.

$$Ut_{\%m_{0,i+e}}(t) = \frac{M_{8:10}(t)}{M_{8:10}(t) + M_{6:7}(t)} \times 100\% \quad (\text{Eq.17})$$

$$\int_{t_0}^{t_1} U' t_{\%m_0} dt = \frac{\int_{t_0}^{t_1} S_{0,1}(t) dt}{\int_{t_0}^{t_1} S_{0,1}(t) dt + \int_{t_0}^{t_1} S_{0,6,7}(t) dt} \times 100\% \quad (\text{Eq.18})$$

## Measurement of End Metabolites $m_{8:10}$ and $m_{6:7}$

Although the equations above may seem tedious, they will be solved using simple concentration measurements of 7 metabolites of vitamin D from plasma and from a 24-hour urine sample (including the currently common measurement of plasma  $m_0$ ,  $25(\text{OH})\text{D}_3$  and  $m_1$ ,  $1,25(\text{OH})_2\text{D}_3$ ). The 7 required metabolite concentration measurements include:

$m_0$  –  $25(\text{OH})\text{D}_3$  – precursor of active vitamin  $\text{D}_3$  - used now to evaluate vit. D status)

$m_1$  –  $1,25(\text{OH})_2\text{D}_3$  – active vitamin D (currently available)

$m_6$  –  $25,26,27$ - Trinorcholecalciferol- $24$ -carboxylic acid – non  $m_1$  inactive end metabolite of  $m_0$

$m_7$  –  $25(\text{OH})\text{D}_3$ - $26$ - $23$  Lactone – non  $m_1$  inactive end metabolite of  $m_0$

$m_8$  –  $1$ - $\text{OH}$ - $23$ - $\text{COOH}$ - $24,25,26,27$  Tetranor  $\text{D}_3$  – inactive end metabolite of  $m_1$

$m_9$  –  $1,25\text{R},(\text{OH})_2\text{D}_3$ - $26$ - $23\text{S}$  – inactive end metabolite of  $m_1$

$m_{10}$  –  $23$ - $\text{COOH}$ - $24,25,26,27$  Tetranor  $\text{D}_3$  – inactive end metabolite of  $m_1$

Note: See figures 2a and 2b

This molar balance approach depends on the accurate and standardized measurement of the serum end metabolites of active vitamin D and of the diverted end metabolites of its precursor,  $25(\text{OH})\text{D}_3$ . These measurements are the critical foundation of this method. Serum, which is plasma with platelets and clotting factors removed, is used to make these measurements. The serum samples will be formed by spinning down a whole blood sample after clotting has occurred in order to separate the serum from the blood sample cells, platelets, and clotting factors.

Liquid-chromatography-tandem-mass spectrometry (LC-MS-MS) is considered the measurement of choice for vitamin D metabolites.<sup>49,50</sup> With LC-MS-MS up to twelve vitamin D metabolites have been measured simultaneously.<sup>51,52</sup> Analytical challenges exist with this technology. Sample type, protein precipitation, analyte extraction, derivatization, chromatographic separation ionization, and capabilities of the mass spectrometer must be addressed.<sup>49</sup> Calibration, standardization, and use of internal standards are also important requirements to achieve consistent, accurate results.

Purified standard compounds for only two of the three end metabolites of active vitamin D,  $m_8$ , calcitric acid, and  $m_{10}$ , calcioic acid are available commercially.<sup>53</sup> A purified standard compound for the remaining end metabolite of active vitamin D,  $m_9$ , or calcitriol- $26,23$ -lactone and standard compounds for the diverted,  $m_0$  precursor, end metabolites,  $m_6$  or cholacalcioic acid and  $m_7$  or  $25(\text{OH})\text{D}_3$ - $26$ - $23$  lactone will have to be synthesized since these standard compounds are required for the liquid-

chromatography-tandem-mass spectrometry measurements of these serum end metabolite measurements.

About 90% of circulating 25(OH)D<sub>3</sub> is protein bound to vitamin D binding protein (VDBP), albumin, and lipoproteins.<sup>49</sup> The percent binding of active vitamin D end metabolites, and the diverted vitamin D precursor end metabolite, to serum VDBP may not be known. The binding of end metabolites and their relative fat and water solubilities may have to be determined. Measurement of the three end metabolites of active vitamin D and the two end metabolites of the precursor, 25(OH)D<sub>3</sub> which are diverted away from the synthesis of active vitamin D, may also depend on their actual concentrations in plasma and urine and the range of measurability. The measurements of these end metabolites would be made using the same instruments that are currently measuring other forms of vitamin D.

A source of human CYP24A1 hydroxylase enzyme will be needed to further evaluate and test the proposed assays used by this model. This enzyme will be used to drive the intermediate metabolites to their end metabolites. This reagent (enzyme) will be required to verify that there is not a significant change in total intermediate metabolites during a transitory increase or decrease in active vitamin D synthesis or in the rate of vitamin D precursor diversion. This enzyme is currently available from several commercial sources according to Biocompare.com.<sup>54</sup> CYP24A1 has been used in previous vitamin D metabolic studies.<sup>55</sup>

Vitamin D metabolite measurements have also been made from human spot urine specimens including 25(OH)D<sub>3</sub> and 24,25(OH)<sub>2</sub>D<sub>3</sub>.<sup>22</sup> Measurement of human spot urine 1,25(OH)<sub>2</sub>D<sub>3</sub> and 23,25(OH)<sub>2</sub>D<sub>3</sub> concentrations were below the limits of detection. The normal volume range of an adult 24-hour urine is 800-2000 with a normal intake of 2 liters of fluid per day. Since the 24-hour urine can be concentrated, concentrating the urine will make the detection of end metabolites in urine easier.

Finally, the technologies used in measuring or monitoring vitamin D metabolites, although challenging, are well established. The only new aspect is adding 5 different end metabolites of vitamin D to the two currently dominant forms of vitamin D measured, (i.e., active vitamin D<sub>3</sub>, 1,25(OH)<sub>2</sub>D<sub>3</sub> and its immediate precursor, 25(OH)D<sub>3</sub>).

## **How Can and Why Should These Vitamin D Parameters be Used?**

Using a molar balance model approach the following vitamin D parameters can be calculated: 1) an estimate of active vitamin D synthesis in the body at any time (t) and over a 24-hour time interval, 2) an active vitamin D demand ratio, and 3) an active vitamin D % utilization. Clinical

lab software will perform the calculations listed in equations 9 through 18 using the measured concentrations of the end metabolites  $m_{8:10}$  and  $m_{6:7}$  as well as different constants for men and women. Each of these new vitamin D parameters can then be determined and monitored in many different conditions where the demand by the body for active vitamin D changes dramatically. These parameters cannot be currently determined by simply measuring serum  $25(\text{OH})\text{D}_3$  and  $1,25(\text{OH})_2\text{D}_3$  levels in the serum.

During severe infections caused by many different agents including the SARS-CoV-2 virus, the immune system may require significantly greater synthesis of active vitamin D to suppress the offending agent (i.e., virus) and the inflammatory response caused by the agent.<sup>56</sup> These clinical vitamin D parameters along with other measurements of an individual's clinical response to their COVID-19 infection will assist clinicians to establish when significant additional vitamin D supplementation is helpful and to determine the required type and dose of vitamin D supplementation.

Until these new vitamin D parameters are available, software has been developed and is available online to determine/calculate annual mean serum  $25(\text{OH})\text{D}_3$  levels as well as seasonal trough and peak values, "25 Hydroxyvitamin D Calculator for Seasonal Adjustment", developed at the Kidney Research Institute, University of Washington.<sup>57,58</sup> This software/app has proved to be quite clinically useful in adjusting vitamin D supplementation based on the time of year that patients, with chronically low vitamin D status, have their vitamin D levels drawn.

A second online software/app, "Vitamin D Calculator", has been developed by the GrassrootsHealth Nutrient Research Institute and is available online to determine the dose of cholecalciferol ( $\text{D}_3$ ) needed to increase the serum level of  $25(\text{OH})\text{D}_3$  level from a lower level to a higher level either quickly (over about 1-2 weeks) using a loading dose followed by an increased daily dose or more slowly over 2-3 months using only an increased daily dose.<sup>59-62</sup>

Finally, until these vitamin D parameters are available, another strategy that has not been yet reported, is to use active vitamin D supplementation acutely to maximize the viral suppression and inflammatory moderating properties of the active form of vitamin D. The advantage of this form of vitamin D is its immediate activity against a virus and its fast half-life (hours) in contrast to the long half-lives of conversion of  $\text{D}_3$  (weeks) and  $25(\text{OH})\text{D}_3$  (days) to active vitamin D. This approach may be more important in those who have high body mass indices and low  $25(\text{OH})\text{D}_3$  storage reflected by low serum levels.

## **Molar Balance Model Limitations**

The molar balance model depends on several assumptions some of which may need modification as the end metabolites are initially measured and some of the assumptions will

not be accurate in all situations. If the extracellular volume or plasma volumes change significantly due to swelling, the assumed volume values will have to be modified. Kidney failure will also prevent the measurement of end metabolites in the urine and may lead to build up of some end metabolites in the body including the extracellular compartment and plasma, and to greater excretion of these metabolites in the stool.

## Summary and Conclusions

A molar balance model is proposed to determine total body active vitamin D,  $m_1$ , levels including synthesis over a 24-hour period, the level of demand in an individual for active vitamin D, and the % utilization of vitamin D precursor,  $m_0$ , to synthesize active vitamin D. Determination of these parameters associated with vitamin D levels and synthesis will require the new measurement of end vitamin D metabolites  $m_{6:10}$  in both serum and urine. Knowing this new information may enable clinicians to improve the body's immune system response to COVID-19 viral infections as well as to other viruses going forward by maximizing the positive effects of active vitamin D on immune system function.

Because cells/tissues of the body (especially immune system cells) sometimes have dramatically changing requirements for active vitamin D, there may not be a consistent stored amount of vitamin D (as measured by plasma 25(OH)D<sub>3</sub> levels) or single minimum daily requirement to insure a sufficient amount of active vitamin D synthesis in all circumstances. Knowing the total active vitamin D that has been synthesized at one point in time or that has been synthesized over 24 hours, knowing the demand ratio for active vitamin D<sub>3</sub>, and knowing the % utilization of  $m_0$  for the synthesis of active vitamin D may improve our understanding of how to dose active vitamin D and active vitamin D precursor supplementation. This new method of determining vitamin D requirements may help to determine changing requirements for active vitamin D at any given time or in different situations the body may encounter. Suppression of COVID-19 replication by adequate levels of active vitamin D may not only reduce the effect of the virus on an individual but may also lower the level of contagiousness of an individual with a COVID-19 virus infection as well as slow the spread of the virus by lowering the positivity rate within a community.<sup>63</sup>

Serum 25(OH)D<sub>3</sub> vitamin D levels have a quite large normal range in the body without toxic side effects and the body has a way to eliminate excess vitamin D precursor to a significant degree. (See yellow oval in the vitamin D metabolic pathways shown in Figure 2b.) If an optimal range of active vitamin D to suppress the COVID-19 virus could be determined, then the type and level of vitamin D supplementation along with vaccination could more easily be determined to mitigate COVID-19 morbidity and mortality and to protect human beings from other viruses going forward.

Figure 1: Model for Absorption, Synthesis, Transport, Conversion, Storage, and Excretion of vitamin D Precursors and Metabolites by the Body

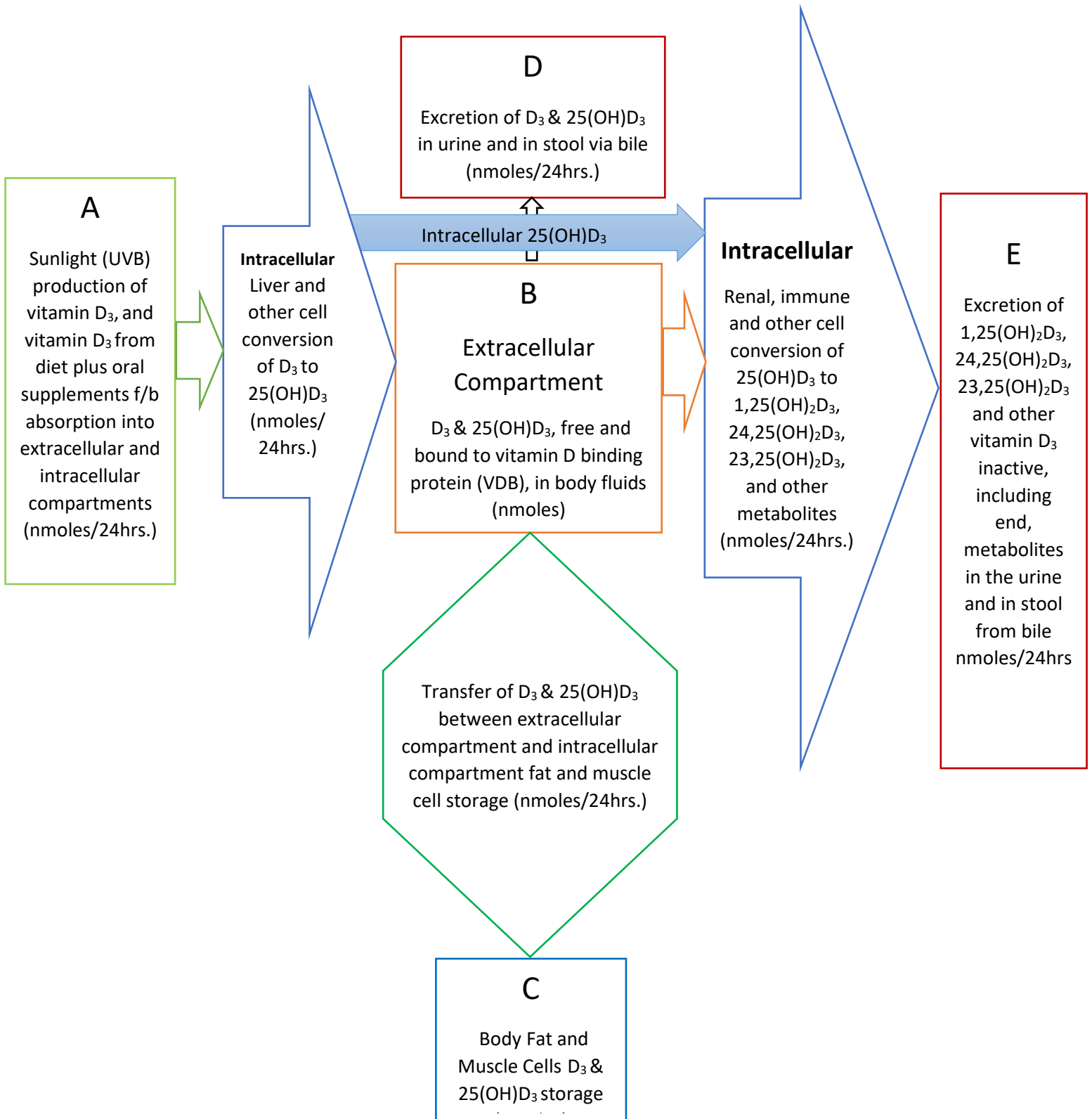


**Figure 2a: Intracellular Vitamin D Pathways Describing the Conversion of 25(OH)D<sub>3</sub>, m<sub>0</sub>, to Its Initial and End Metabolites, m<sub>n</sub>**

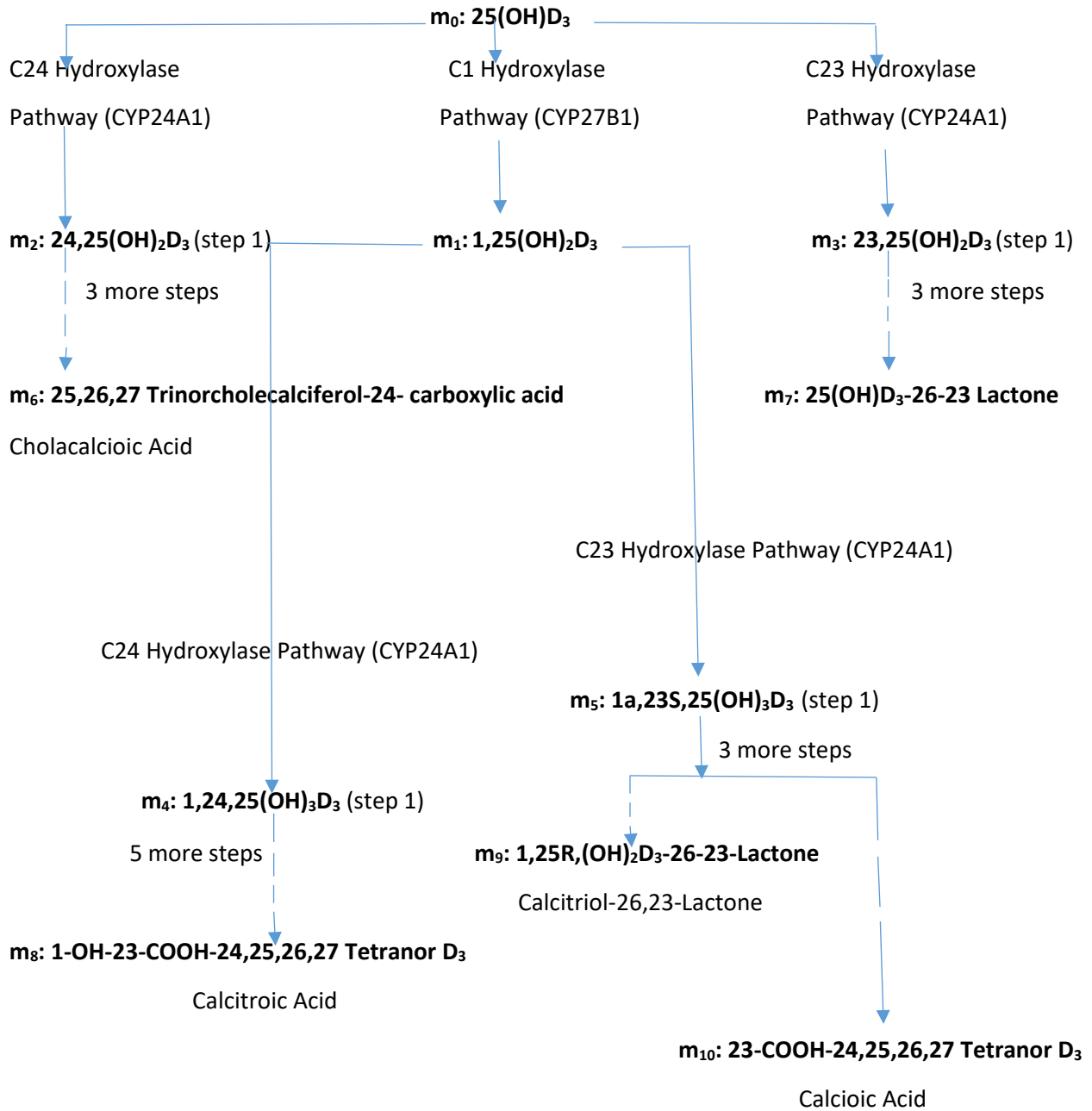


**Fig. 2a Cont'd**

Note: **C#** in front of the enzymes represents the carbon atom location which is acted upon by the pathway enzyme. The  $m_n$  terms describe the initial and end metabolites of  $m_0$ . The end metabolites ( $m_6$  to  $m_{10}$ ) pass from the intracellular to the extracellular compartments and are excreted in urine (approx. 25%) and in stool (approx. 75%).

**Fig. 2b Simplified Flow Diagram of the Intracellular Metabolism of 25(OH)D<sub>3</sub>, m<sub>0</sub>, to Its Initial Metabolites (m<sub>1</sub>, m<sub>2</sub>, & m<sub>3</sub>), and End Metabolites (m<sub>4</sub> & m<sub>5</sub>) and (m<sub>6</sub> to m<sub>10</sub> through m<sub>1</sub>)**

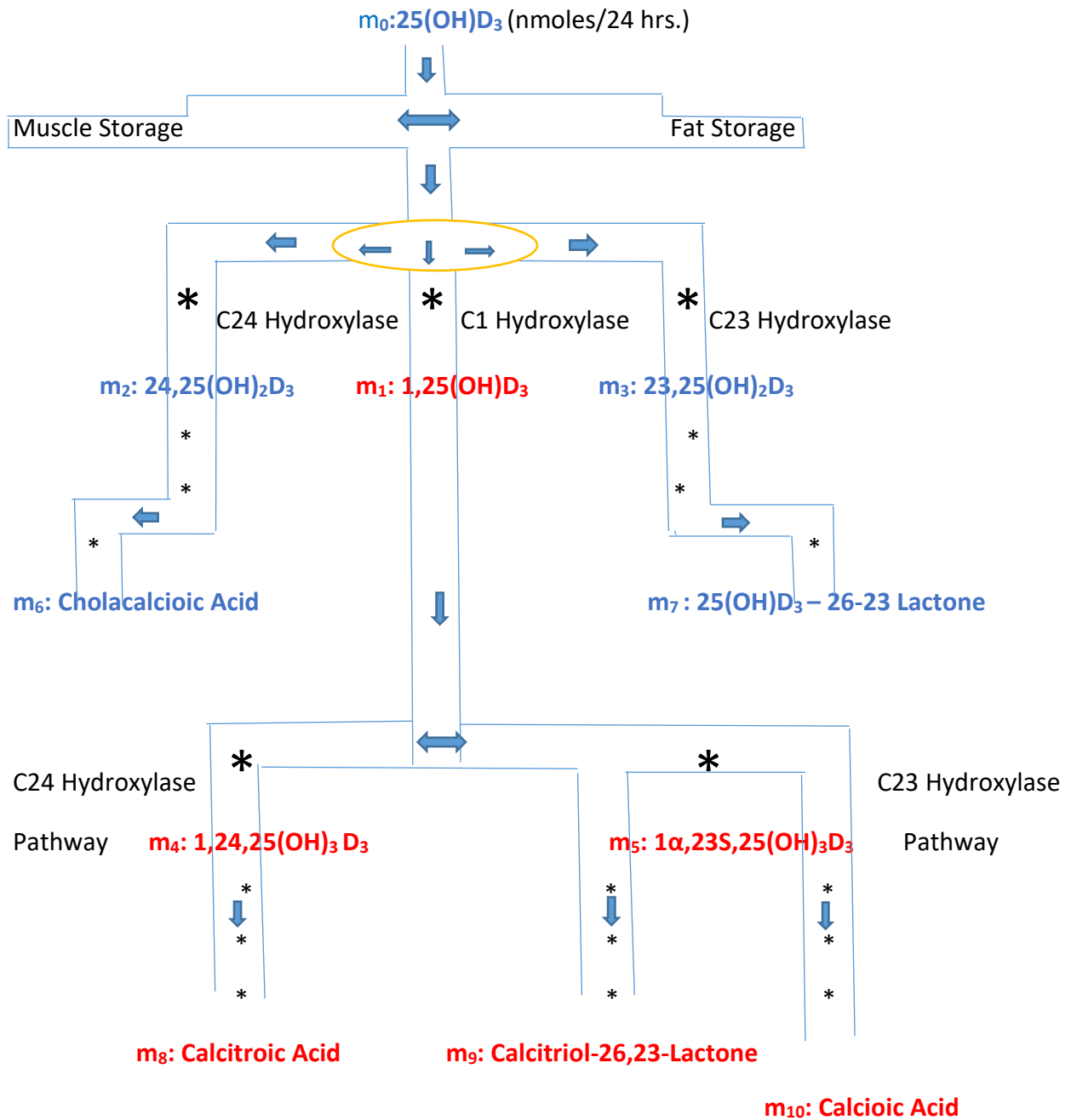


Figure 2b cont'd: In this flow diagram, the  $m_n$  terms represents the initial and end metabolites of  $m_0$  (i.e.  $m_1$  through  $m_{10}$ ). The large bold \*symbols represent the enzymes for the synthesis of the initial and end metabolites of  $m_0$  ( $25(\text{OH})\text{D}_3$ ). The initial three \* symbols can be thought of as valves which can regulate the amount of active vitamin D hormone,  $m_1$ , synthesized or the amount of  $m_0$  diverted away from  $m_1$  synthesis in response to a changing need by the body for active vitamin D at any given moment in time or for any given changing situation. Red metabolites represent the active vitamin D pathway to its end metabolites. Blue metabolites are those of  $25(\text{OH})\text{D}_3$  which are diverted away from the synthesis of active vitamin D,  $m_1$ .

**Figure 2c: Simpler Model of the Body's Synthesis, Transport, and Excretion of  $m_0$  [25(OH)D<sub>3</sub>],  $m_1$  [1,25(OH)<sub>2</sub>D<sub>3</sub>] and their End Metabolites,  $m_6$  to  $m_{10}$  (nmoles/24hrs.)**

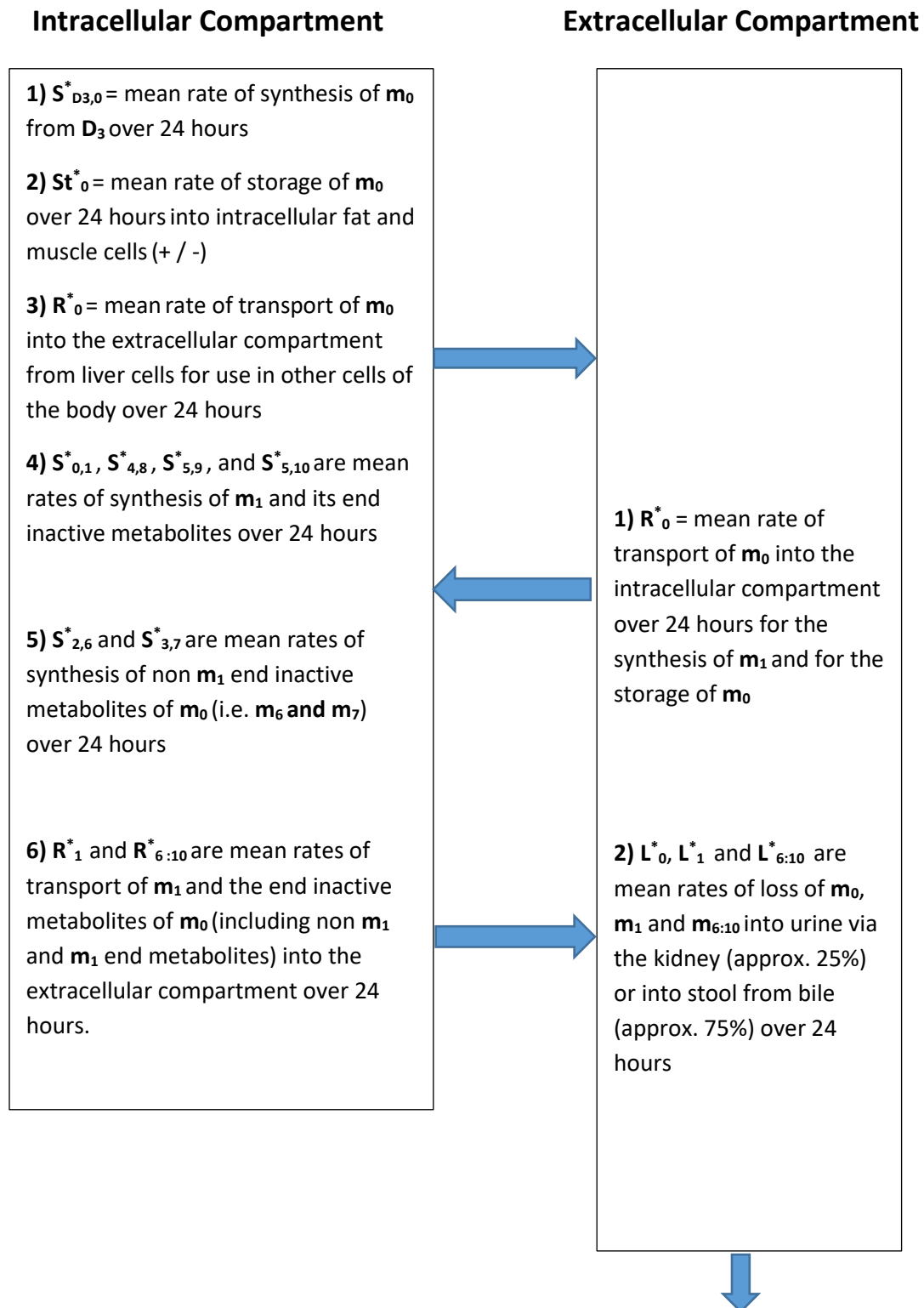


Figure 2c cont'd.

### Intracellular and Extracellular Compartment Volume Analysis

Water makes up approximately 60% of body weight in the male and 55% body weight in the female

For a 55kg female:

1. Extracellular Compartment Volume ( $V^e$ ) = 's about 11 liters [including plasma volume ( $V^{pla}$ ) 2.5 liters, + Interstitial volume ( $V^{inter}$ ) 8.5 liters + transcellular volume ( $V^{trans}$ ) .4 liters –aver.]
2. Intracellular Compartment Volume ( $V^i$ ) = 's about 22 liters
3.  $V^i$  = 's about  $2V^e$  and in females  $V^e$  equals about  $4.4V^{pla}$  Ref. 44
4. Approx. mean HCT 40% (range 36-44%)  
[my.clevelandclinic.org/health/diagnostic17683-hematocrit/results-and-follow-up](http://my.clevelandclinic.org/health/diagnostic17683-hematocrit/results-and-follow-up)  
assessed Mar 8, 2020

For a 70 Kg Male:

5. Extracellular Compartment Volume ( $V^e$ ) = 's about 14 liters [including plasma volume ( $V^{pla}$ ) 3.0 liters, + Interstitial volume ( $V^{inter}$ ) 10.5 liters + transcellular volume ( $V^{trans}$ ) .5 liters –aver.]
6. Intracellular Compartment Volume ( $V^i$ ) = 's about 28 liters
7.  $V^i$  = 's about  $2V^e$  and in males  $V^e$  equals about  $4.66V^{pla}$  Ref. 45
8. Approx. mean HCT 45.5% (range 41-50%)  
[my.clevelandclinic.org/health/diagnostic17683-hematocrit/results-and-follow-up](http://my.clevelandclinic.org/health/diagnostic17683-hematocrit/results-and-follow-up)  
assessed Mar 8, 2020

Differences between average male and female volumes are as follows:

Plasma volume – males have 20% greater volume based on average size

Extracellular volume – males have 27% greater volume based on average size

Intracellular volume – males have 27% greater volume based on average size

Because of the differences in mean % hematocrit as well as physical size between men and women, the total % difference in aqueous volume (extracellular + intracellular) between men and women would be a difference of  $42L/33L \times 100\%$  or 127%

Figure 2c cont'd.

For males  $V_{e+1} = 42L$  and for females  $V_{e+1} = 33$

$$V_i = 28L$$

$$V_i = 22L$$

$$V_e = 14L$$

$$V_e = 11L$$

$$V_p = 3L$$

$$V_p = 2.5L$$

**Figure 2d: Simplest Model of the Body's Composition of Non  $m_1$  End Metabolites from  $[25(OH)D_3]$ ,  $m_6$  &  $m_7$  (\*), and End Metabolites from  $m_1$   $[1,25(OH)_2 D_3]$ ,  $m_8 - m_{10}$ (+), at any point in time,  $t$ , in nmoles**

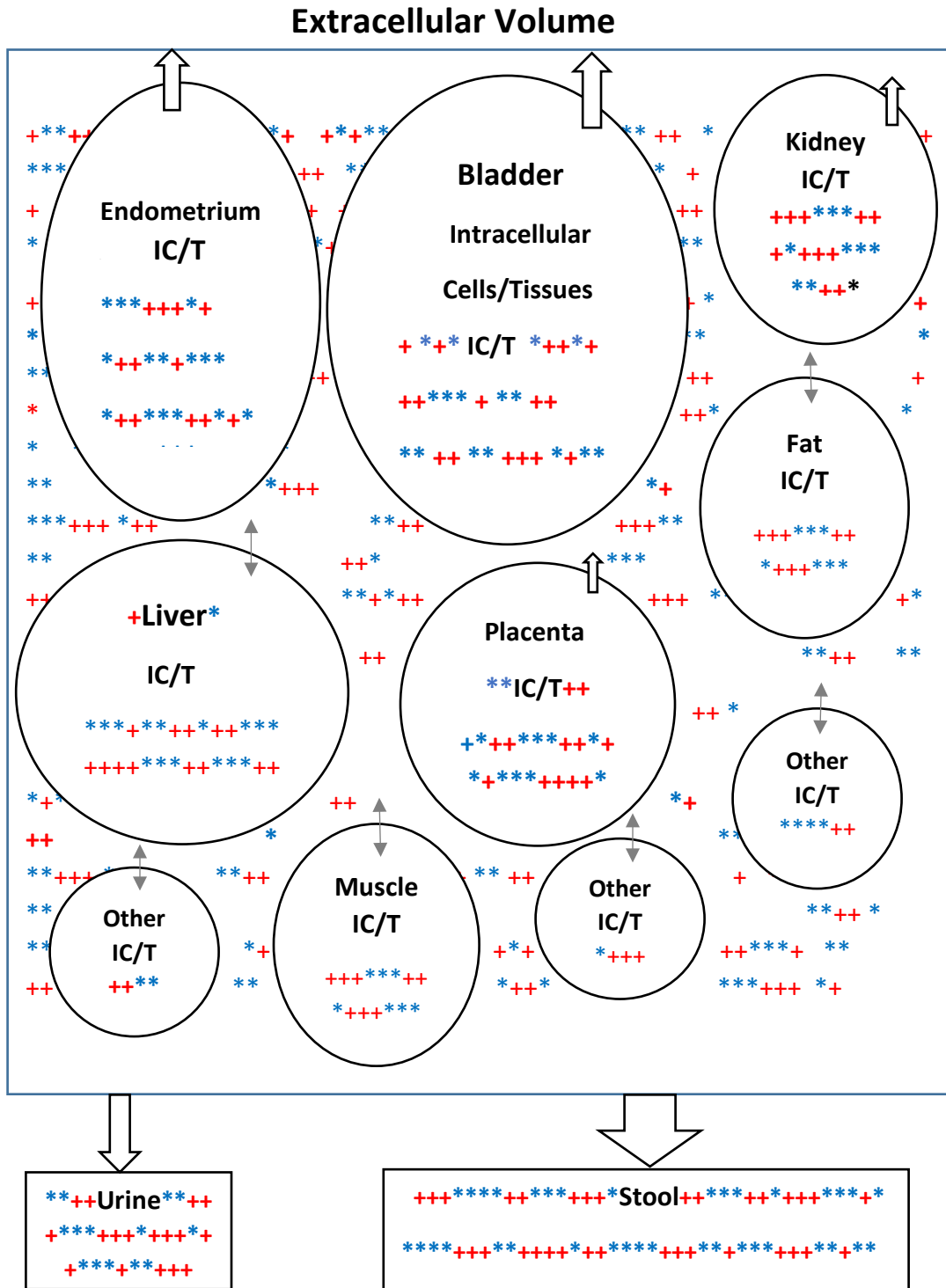


## Figure 2d Cont'd

Note: Arrows indicate direction of flow of end metabolites. Unidirectional arrows indicate flow from consistently high concentration to low (i.e. cells synthesizing end metabolites). Bidirectional arrows indicate passive flow into and out of cells where there is no significant synthesis of end metabolites of  $m_0$  and  $m_1$ .

# Appendix A. Molar Balance Model Derivation

## 1. Definitions

### 1.0 List of included vitamin D $m_n$ metabolites:

- $m_{D_3}$  –  $D_3$  – precursor of  $m_0$  (Figure 2c only)
  - $m_0$  – 25(OH) $D_3$  – precursor of active vitamin  $D_3$
  - $m_1$  – 1,25(OH) $_2D_3$  – initial active vitamin  $D_3$  metabolite of  $m_0$
  - $m_2$  – 24,25(OH) $_2D_3$  – an initial inactive metabolite of  $m_0$
  - $m_3$  – 23,25(OH) $_2D_3$  – an initial inactive metabolite of  $m_0$
  - $m_4$  – 1,24,25(OH) $_3D_3$  – an initial inactive metabolite of  $m_1$
  - $m_5$  – 1 $\alpha$ ,23S,25(OH) $_3D_3$  – an initial inactive metabolite of  $m_1$
  - $m_6$  – 24-COOH-25,26,27 Trinor  $D_3$  – non  $m_1$  inactive end metabolite of  $m_0$
  - $m_7$  – 25(OH) $D_3$ -26-23 Lactone – non  $m_1$  inactive end metabolite of  $m_0$
  - $m_8$  – 1-OH-23-COOH-24,25,26,27 Tetranor  $D_3$  – inactive end metabolite of  $m_1$
  - $m_9$  – 1,25R,(OH) $_2D_3$ -26-23S – inactive end metabolite of  $m_1$
  - $m_{10}$  – 23-COOH-24,25,26,27 Tetranor  $D_3$  – inactive end metabolite of  $m_1$
- Note: See figures 2a and 2b

### 1.1. Metabolite quantities and concentrations. The quantity of vitamin D metabolites at time $t$ are denoted

$$m_{n,k}(t), \tag{D.1}$$

where the first subscript,  $n$ , indexes metabolite type (see list above for metabolite definitions) and the second subscript,  $k$ , designates three dimensional spaces in which metabolites can be located. There are four primary spaces or compartments: intracellular, extracellular, plasma, and collected urine. The plasma space is a sub-compartment of the extracellular space. Two secondary spaces used in the mathematical derivation include the body's stool space and the space or volume of the collected plasma samples used to make metabolite measurements. The spaces are denoted as follows:

- (1)  $k = i$  for intracellular space
- (2)  $k = e$  for extracellular space
- (3)  $k = p$  for plasma sub-extracellular space
- (4)  $k = u$  collected urine space
- (5)  $k = s$  collected stool space
- (6)  $k = cp$  collected plasma sample

Note: number subscripts always refer to metabolites or time and letter subscripts to spaces.

The total body nmoles of metabolite  $m_n$  at any time (t) in the intracellular and extracellular compartments is denoted:

$$M_{n,i+e}(t) \tag{D.2}$$

The total nmoles of metabolite  $m_n$  over any time period ( $t_1 - t_0$ ) in a urine collected specimen is denoted:

$$M_{n,u}(t_1) - M_{n,u}(t_0) = M_{n,u}(t_1) \tag{D.3}$$

Since the nmoles at the start of a urine collection will always be = to 0

Metabolite concentrations in each space are defined as:

$$C_{n,k}(t) = \frac{m_{n,k}(t)}{V_k} \tag{D.4}$$

where  $V_k$  is the volume in compartment k.

## 1.2 Metabolite transport, synthesis, and loss.

The transport rate of any metabolite n from the intracellular to extracellular compartment (space) at time (t) is

$$R_n(t) \tag{D.5}$$

We consider several pathways of vitamin D metabolite synthesis and use S to denote rates of synthesis/conversion. All synthesis/conversion occurs in the intracellular compartment. The rate of synthesis/conversion between metabolites i and j, where  $i \neq j$ , is denoted

$$S_{i,j}(t) \tag{D.6}$$

Some specific synthesis rates of interest are:

$$S_{0,1}(t): \text{synthesis rate of metabolite } m_1 \text{ from metabolite } m_0 \tag{D.7}$$

$$S_{4,8}(t), S_{5,9}(t), \text{ and } S_{5,10}(t): \text{synthesis rates of the end metabolites of } m_1 \text{ from the first intermediate metabolites of } m_1. \tag{D.8}$$

$S_{0,2}(t) + S_{0,3}(t) = S_{0,2:3}(t)$  equals the synthesis rate of intermediate metabolites  $m_2 + m_3$  ( $m_{2:3}$ ) from metabolite  $m_0$  (D.9)

(Note:  $S_{0,2:3}(t)$  denotes synthesis rate of the first intermediate metabolites of  $m_0$  diverted away from the synthesis of active vitamin D,  $m_1$ .)

$S_{2,6}(t)$  and  $S_{3,7}(t)$ : synthesis rate of the end metabolites of  $m_0$  diverted away from the synthesis of  $m_1$  (D.10)

One goal of this model is to develop a method for measuring the synthesis of the active vitamin D metabolite,  $m_1$ . Using our notation, the total quantity of  $m_1$  synthesized from  $m_0$  between two arbitrary time periods  $t_0$  and  $t_1$  is

$$\int_{t_0}^{t_1} S_{0,1}(t) dt \quad (D.11)$$

### 1.3. Metabolite loss and urine volume creation.

The total loss of metabolite  $m_n$  from the extracellular space is divided between the urine volume space, 25% and the stool volume space 75%. Total rate of metabolite,  $m_n$ , loss:

$$L^*_n(t) = L_{n,u}(t) + L_{n,s}(t) = 4L_{n,u}(t) \quad (D.12)$$

and we denote the rate of urine volume creation at time  $t$  as

$$U(t) \quad (D.13)$$

The collected urine volume consists of a urine volume created between the time at which collection starts,  $t_s$  or  $t_0$ , and the time at which collection ends,  $t_e$  or  $t_1$ . Clinically the urine volume is always 0 at the start of a urine collection therefore terms involving  $t_s$  or  $t_0$  always drop out.

$$V_u(t_1) - V_u(t_0) = V_u(t_1) = \int_{t_0}^{t_1} U(t) dt \quad \text{since } V_u \text{ at the start of collection is 0} \quad (D.14)$$

The quantity of metabolite  $m_n$  in the urine space at the end of the collection period consists of 25% of metabolites  $m_n$  excreted from the body between the time at which collection starts,  $t_s$  or  $t_0$ , and the time at which collection ends,  $t_e$  or  $t_1$ . ( Note: the remaining 75% of metabolite excretion occurs through the stool.) Therefore, we can write

$$m_{n,u}(t_1) - m_{n,u}(t_0) + m_{n,s}(t_1) - m_{n,s}(t_0) = \int_{t_0}^{t_1} L_n^*(t) dt = 4 \int_{t_0}^{t_1} L_{n,u}(t) dt$$

Since  $m_{n,u}$  at the urine collection start time ( $t_0$ ) is 0 and  $[m_{n,s}(t_1) - m_{n,s}(t_0)] = 3m_{n,u}(t_1)$  then:

$$m_{n,u}(t_1) + [m_{n,s}(t_1) - m_{n,s}(t_0)] = 4[m_{n,u}(t_1)] = 4 \int_{t_0}^{t_1} L_{n,u}(t) dt \quad (D.15)$$

The concentration of metabolite  $n$  in the urine space at the end of the collection period is also a function of the end collection time only since the nmoles of  $m_n$  and urine volume equal 0 at the start of the urine collection ( $t_0$ ):

$$C_{n,u}(t_1) = \frac{m_{n,u}(t_1)}{V_u(t_1)} = \frac{\int_{t_0}^{t_1} L_{n,u}(t) dt}{\int_{t_0}^{t_1} U(t) dt} \quad (D.16)$$

#### 1.4 $m_1$ Demand Ratio

The  $1,25(\text{OH})\text{D}_3$ ,  $m_1$ , demand ratio expresses the ratio of the sum of end inactive metabolites of active vitamin D,  $1,25(\text{OH})_2\text{D}_3$ ,  $m_1$  (i.e.  $m_8 + m_9 + m_{10}$ ) to the sum of non  $m_1$ , end inactive metabolites of  $25(\text{OH})\text{D}_3$  (i.e.  $m_6 + m_7$ ) in the intracellular plus extracellular compartments at some point in time, ( $t$ ).

$$\text{Drm}_{1,i+e}(t) \quad (D.17)$$

Note: If the sum of  $m_6 + m_7$  in the denominator cannot be measured or if it becomes very small causing the ratio to become very large, then the denominator can become  $1 \times 10^{-9} + m_6 + m_7$ .

### 1.5 $m_0$ Percent Utilization

At any point in time(t), the 25(OH)D<sub>3</sub>,  $m_0$ , percent utilization equals the sum of end inactive metabolites of active vitamin D, 1,25(OH)<sub>2</sub>D<sub>3</sub>,  $m_1$  (i.e.  $m_8$ , +  $m_9$ , +  $m_{10}$ ) divided by the sum of end inactive metabolites of active vitamin D, 1,25(OH)<sub>2</sub>D<sub>3</sub>,  $m_1$  (i.e.  $m_8$ , +  $m_9$ , +  $m_{10}$ ) plus the sum of the end inactive metabolites of  $m_0$  (i.e.  $m_6$  +  $m_7$  or the end metabolites that are diverted away from the synthesis of  $m_1$ ) multiplied by 100%.

$$Ut_{\%m_0,i+e}(t) \quad (D.18)$$

The rate of change of  $m_0$  percent utilization is defined as:

$$Ut'_{\%m_0,i+e}(t) \quad (D.19)$$

## 2. Assumptions

Plasma volumes are somewhat different between men and woman based on different physical sizes (average woman 55 kg and average male 70 kg) and they have slightly different mean hematocrit % (Hct. %) levels (mean for women 40% and mean for men 45.5 %). Thus, the average plasma volume for a 55kg woman is 2.5 L and for an average 70kg male 3.0 L. An average male's plasma volume is thus 20% greater than a women's plasma volume. See figure 2c. for more detailed explanation of volume determinations.

For the purpose of this model, the plasma, extracellular, and intracellular volumes are assumed to be known constants for the average female 155kg and the average male 170 kg, denoted as  $V_p$ ,  $V_e$ , and  $V_i$ . The intracellular and extracellular volumes can be expressed as multiples of the plasma volume:

$$V_p = \text{constant} = 3.0L \text{ for men and } 2.5 \text{ L for women (Ref. 29,30)} \quad (A.1)$$

$$V_e = \text{constant} = 4.66V_p \text{ for men and } 4.4V_p \text{ for women} \quad (A.2)$$

$$V_i = \text{constant} = 9.32V_p \text{ for men and } 8.8V_p \text{ for women} \quad (A.3)$$

For this model the total nmoles of vitamin D metabolites,  $m_n$ , in the intracellular and extracellular compartments or spaces will be determined from measurement of metabolite  $m_n$  concentrations in a collected plasma sample.

The next assumption is that metabolite concentrations of  $m_n$  in the extracellular, plasma, and collected plasma sample are equal at the time (t) of specimen collection, i.e.,

$$C_{n,e}(t) = C_{n,p}(t) = C_{n,cp}(t) \quad (A.4)$$

Mean metabolite concentrations in the intracellular and extracellular compartments are assumed to be proportional with a constant of proportionality of  $\beta$ .  $\beta$  equilibrates the mean concentrations of  $m_n$  metabolites between the non-homogeneous intracellular and assumed approximately homogeneous extracellular compartments. End metabolites of  $m_0$  and  $m_1$  are assumed to transfer passively from the intracellular to the extracellular compartment and visa versa passively depending on concentration gradients.  $\beta$  is assumed to be a constant over physiological concentrations of end metabolites,  $m_n$ , and to be somewhat greater than 1 since a mean higher to lower concentration gradient overall between the intracellular and extracellular spaces must exist in order for the end metabolites to be excreted from the body. Initially  $\beta$  will be assumed to be 1.1 – see figure 2d.

$$C_{n,i}(t) = \beta C_{n,e}(t) \quad \text{and therefore}$$

$$C_{8:10,i}(t) = \beta C_{8:10,e}(t) = \beta C_{8:10,cp}(t) \quad \text{and} \quad (\text{A.5})$$

$$C_{6:7,i}(t) = \beta C_{6:7,e}(t) = \beta C_{6:7,cp}(t) \quad (\text{A.6})$$

Assumption A.7 below assumes that the rate of synthesis of  $m_1$  from  $m_0$  is the same as the sum of the rates of synthesis of its three end metabolites. [i.e. Every time 12 molecules of  $m_1$  are synthesized a total of 12 molecules of end metabolites of  $m_1$ , ( $m_8 + m_9 + m_{10}$ ), will also be synthesized. Similarly, A.8 assumes that the sum of the rates of synthesis of  $m_2$  from  $m_0$  and  $m_3$  from  $m_0$  is the same as the sum of the rates of synthesis of  $m_6$  from  $m_2$  and  $m_7$  from  $m_3$

$$S_{0,1}(t) = S_{4,8}(t) + S_{5,9}(t) + S_{5,10}(t) \quad (\text{A.7})$$

$$S_{0,2:3}(t) = S_{2,6}(t) + S_{3,7}(t) \quad (\text{A.8})$$

Assumptions A.7 and A.8 do not reflect what is truly going on in the two intracellular vitamin D  $m_0$  pathways because these assumptions neglect possible changing concentration levels and the presence of changing nmoles of  $m_n$  intermediate metabolites. Assumption A.7 assumes that the rate of active vitamin D synthesis equals the sum of the rate of end metabolite synthesis (a presumed steady state) without a buildup or decrease in intermediate metabolites. Assumption A.8 likewise assumes that the rate of  $m_0$  diversion away from active vitamin D synthesis equals the sum of the rate of its end metabolite synthesis (a presumed steady state) without a buildup or decrease in its intermediate metabolites. Even under non steady state conditions these two assumptions might introduce a tolerable error.

The validity of A.7 and A.8 assumptions can be checked by doing second serum and urine assays which measures total end metabolites of active vitamin D precursor, active vitamin D, and all of their intermediate metabolites after all active vitamin D precursor, active vitamin D, and its intermediate metabolites are driven to their end metabolites by excess CYP24A1 hydroxylase enzyme added to a second plasma sample drawn at time  $t_0$  and  $t_1$  as well as by a second determination from the urine specimen collected over 24 hours. If, after subtracting out the end metabolites which would have been generated by the remaining active vitamin D and its precursor in the first sample, the measured nmoles of end metabolite in the second sample are significantly larger than those in the first serum sample, then a correction factor can be added to the calculation to account for a buildup of intermediate metabolites in either the  $25(\text{OH})\text{D}_3$  or  $1,25(\text{OH})_2\text{D}_3$  degradation pathways when the synthesis of active vitamin D increases.

The collected serum plasma sample can be divided into two equal parts. In the first part, concentrations of  $C_{0,\text{cp}}(\mathbf{t})$  (where the subscript 0 indicates  $25(\text{OH})\text{D}_3$  and cp indicates collected plasma) and  $C_{1,\text{cp}}(\mathbf{t})$  (where the subscript 1 indicates  $25(\text{OH})_2\text{D}_3$ ) of the first collected plasma specimen must be measured along with the concentrations of the end metabolites of  $1,25(\text{OH})_2\text{D}_3$  ( $m_{8-10}$ ) and  $25(\text{OH})\text{D}_3$  ( $m_{6-7}$ ). To the second sample, excess CYP24A1 hydroxylase enzyme is added to completely drive the breakdown of  $25(\text{OH})\text{D}_3$  and  $1,25(\text{OH})_2\text{D}_3$  to their end metabolites.

Then measured concentrations of  $C_{0,\text{cp}}$ ,  $C_{1,\text{cp}}$ ,  $C_{6-7,\text{cp}}$ , and  $C_{8-10,\text{cp}}$  in the first sample must be subtracted from the concentration of  $C_{6-7,\text{cp}}(\mathbf{t})$  plus  $C_{8-10,\text{cp}}(\mathbf{t})$  in the second sample. Any discrepancy between the two values will represent the concentration of intermediate metabolites not measured in the first collected plasma sample. If the discrepancy is significant a correction factor can be introduced to correct for an increase in intermediate metabolites in the  $25(\text{OH})\text{D}_3$  and  $25(\text{OH})_2\text{D}_3$  degradation pathways when the synthesis of either of these vitamin D forms increases significantly. The same assumptions and processes described in this and the above paragraphs can be used in the evaluation of the end metabolites of active vitamin D and its precursor in urine collections. This two-measurement comparison technique along with the following equations could be used to see whether the assumption that the buildup of intermediates in these two degradation pathways is not significant or needs addressing.

### 3. Measurement of active vitamin D ( $m_1$ ) synthesis and of vitamin D precursor ( $m_0$ ) diversion away from active vitamin D synthesis over time interval ( $t_1 - t_0$ )

3.0. From assumptions A.1 to A.10, total  $m_1$  synthesis and the total diversion  $m_0$  away from the synthesis of active vitamin D,  $m_1$ , over an arbitrary time interval ( $t_1 - t_0$ ) can be estimated in men or women using

- (1) Measurement of  $C_{8:10,cp}$  at times  $t_0$  and  $t_1$
- (2) Measurement of  $C_{6:7,cp}$  at times  $t_0$  and  $t_1$
- (3) Measurement of  $C_{8:10,u}$  at time  $t_1$  (since there is no urine when the collection starts)
- (4) Measurement of  $C_{6:7,u}$  at time  $t_1$  (since there is no urine when the collection starts)
- (5) Measurement of  $V_u(t_1)$
- (6) Measurement of  $C_{0,cp}$  at times  $t_0$  and  $t_1$
- (7) Standard values for  $V_i$ ,  $V_e$ , and  $V_p$ , for men and women

An expression for the synthesis of  $m_1$  over an arbitrary time interval ( $t_1 - t_0$ ) is developed in three steps. In the first step, an expression for the change in quantity of  $m_1$  in the body's intracellular and extracellular compartments over the time interval, ( $t_1 - t_0$ ) is derived using  $m_1$ 's end metabolites,  $m_{8:10}$ . In the second step, an expression for the quantity of  $m_1$  excreted or lost to the body in urine and stool over the same time interval is derived using  $m_1$ 's end metabolites,  $m_{8:10}$ . In the third step, the expressions derived in parts 1 and 2 are summed to solve for the total synthesis of active vitamin D,  $m_1$ , based on the assumption that the change in intracellular plus extracellular nmoles of  $m_{8:10}$  over the time interval, plus the loss of  $m_{8:10}$  in the urine and stool over the same time interval will represent a good estimate of the synthesis of  $m_1$  over this time interval. Using the same approach, an expression for the amount of  $m_0$  diverted away from the synthesis of  $m_1$  will be developed using the end metabolites,  $m_{6:7}$ .

3.1. Step 1. Using assumption A.7, we can write

$$\int_{t_0}^{t_1} S_{0,1}(t)dt = \int_{t_0}^{t_1} S_{4,8}(t)dt + \int_{t_0}^{t_1} S_{5,9}(t)dt + \int_{t_0}^{t_1} S_{5,10}(t)dt = \quad (\text{Eq.1})$$

$$\int_{t_0}^{t_1} S_{0,1}(t)dt = m_{8:10,i}(t_1) - m_{8:10,i}(t_0) + \int_{t_0}^{t_1} R_{8:10}(t)dt \quad (\text{Eq.2})$$

Using definition D.15, the total change in metabolites  $m_8$ ,  $m_9$ , and  $m_{10}$  in the extracellular space over the time interval  $(t_1 - t_0)$  is

$$\begin{aligned}
 m_{8:10,e}(t_1) - m_{0,8:10,e}(t_0) &= \int_{t_0}^{t_1} R_{8:10}(t)dt - \int_{t_0}^{t_1} L_{8:10}^*(t)dt \\
 &= \int_{t_0}^{t_1} R_{8:10}(t)dt - 4 \int_{t_0}^{t_1} L_{8:10,u}(t)dt \quad (\text{Eq.3})
 \end{aligned}$$

Equation 3 can then be rearranged to solve for the total transfer of metabolites,  $m_8$ ,  $m_9$ , and  $m_{10}$  from the intracellular to the extracellular space over the time interval  $(t_1 - t_0)$ :

$$\int_{t_0}^{t_1} R_{08:10}(t)dt = m_{8:10,e}(t_1) - m_{8:10,e}(t_0) + 4 \int_{t_0}^{t_1} L_{8:10,u}(t)dt \quad (\text{Eq.4})$$

Substituting the above expression for the total transfer (R) back into equation 2 gives:

$$\int_{t_0}^{t_1} S_{0,1}(t)dt = m_{8:10,i}(t_1) - m_{8:10,i}(t_0) + m_{0,8:10,e}(t_1) - m_{0,8:10,e}(t_0) + 4 \int_{t_0}^{t_1} L_{8:10,u}(t)dt \quad (\text{Eq.5})$$

The terms on the righthand side of equation 5 will be replaced with known quantities (either from quantities that have been measured before such as volumes or from measurements that we can make based on our definitions or assumptions). The first substitution will be for the metabolite loss term involving urine. Note time subscripts  $s$  for start and  $e$  for end have been replaced by 0 for the initial start of the collection where the urine volume and end metabolites of  $m_1$  would be 0 and  $e$  would be replaced by 1 at the end time of the collection. (i.e.  $t_s = t_0$  and  $t_e = t_1$ ). Using definition D.15 and D.16, the total loss of metabolites  $m_8$ ,  $m_9$ , and  $m_{10}$  from the body between  $t_0$  and  $t_1$  (using a factor 4 times the loss from urine to make up for the loss of metabolites from both urine and stool equals:

$$4 \int_{t_0}^{t_1} L_{8:10,u}(t)dt = 4[m_{8:10,u}(t_1)] = 4[C_{8:10,u}(t_1)V_u(t_1)] \quad (\text{Eq.6})$$

Substituting the expression on the righthand side of equation (6) for the metabolite loss term in equation (5) gives:

$$\int_{t_0}^{t_1} S_{0,1}(t)dt = m_{8:10,i}(t_1) - m_{8:10,i}(t_0) + m_{8:10,e}(t_1) - m_{8:10,e}(t_0) + 4[C_{8:10,u}(t_1)V_u(t_1)] \quad (\text{Eq.7})$$

The next step is to determine the expression,  $m_{8:10,i}(t_1) - m_{8:10,i}(t_0) + m_{8:10,e}(t_1) - m_{8:10,e}(t_0)$  in terms of measurable concentrations of  $m_{8:10,cp}$  at time (t) and then substitute the new derived expression into the right side of equation (7).

Note:  $m_{8:10} = m_8 + m_9 + m_{10}$ . Then using assumptions A1- A5, for men

$$m_{8:10,i}(t_1) - m_{8:10,i}(t_0) + m_{8:10,e}(t_1) - m_{8:10,e}(t_0) =$$

$$\frac{\beta[m_{8,p}(t_1) + m_{9,p}(t_1) + m_{10,p}(t_1)]}{V_p} \times 9.32V_p - \frac{\beta[m_{8,p}(t_0) + m_{9,p}(t_0) + m_{10,p}(t_0)]}{V_p} \times 9.32V_p$$

+

$$\frac{m_{8,p}(t_1) + m_{9,p}(t_1) + m_{10,p}(t_1)}{V_p} \times 4.66V_p - \frac{m_{8,p}(t_0) + m_{9,p}(t_0) + m_{10,p}(t_0)}{V_p} \times 4.66V_p$$

equals

$$2\beta \frac{[m_{8,p}(t_1) + m_{9,p}(t_1) + m_{10,p}(t_1)]}{V_p} \times 4.66V_p - 2\beta \frac{[m_{8,p}(t_0) + m_{9,p}(t_0) + m_{10,p}(t_0)]}{V_p} \times 4.66V_p$$

+

$$\frac{m_{8,p}(t_1) + m_{9,p}(t_1) + m_{10,p}(t_1)}{V_p} \times 4.66V_p^{pla} - \frac{m_{8,p}(t_0) + m_{9,p}(t_0) + m_{10,p}(t_0)}{V_p} \times 4.66V_p$$

equals

$$\frac{[(2\beta) + 1] \times [m_{8,p}(t_1) + m_{9,p}(t_1) + m_{10,p}(t_1) - m_{8,p}(t_0) - m_{9,p}(t_0) - m_{10,p}(t_0)] \times 4.66V_p}{V_p}$$

and thus:

$$m_{8:10,i}(t_1) - m_{8:10,i}(t_0) + m_{8:10,e}(t_1) - m_{8:10,e}(t_0) =$$

$$[(2\beta) + 1] \times [C_{8:10,p}(t_1) - C_{8:10,p}(t_0)] \times 4.66V_p$$

(Eq.8)

$$\text{Where } C_{8:10,p}(t) = C_{8,p}(t) + C_{9,p}(t) + C_{10,p}(t) \quad \text{nmoles/L}$$

Substituting the right side of equation 8 into the right side of equation (7) (for men) results in:

$$\int_{t_0}^{t_1} S_{0,1}(t)dt = \{(2\beta) + 1\} \times [C_{8:10,p}(t_1) - C_{8:10,p}(t_0)] \times 4.66V_p + 4[C_{8:10,u}(t_1)V_u(t_1)]$$

$$= 4.66V_p [(2\beta) + 1] \times [C_{8:10,cp}(t_1) - C_{8:10,cp}(t_0)] + 4[C_{8:10,u}(t_1)V_u(t_1)] \quad \text{(Eq.9)}$$

where  $V_p$  for an average size man is 3.0L,  $V_u(t_0) = 0$ , and  $\beta = 1.1$

For women =  $4.4V_p [(2\beta) + 1] \times [C_{8:10,cp}(t_1) - C_{8:10,cp}(t_0)] + 4[C_{8:10,u}(t_1)V_u(t_1)]$  (Eq.10)

where  $V_p$  for an average size woman is 2.5L,  $V_u(t_0) = 0$ , and  $\beta = 1.1$

$t_1$

Similarly, for  $\int_{t_0}^{t_1} S_{0,2,3}(t)dt$  or the amount of  $m_0$  that bypasses the synthesis of  $m_1$

$t_0$  using the same method

=  $4.66V_p [(2\beta) + 1] \times [C_{6:7,cp}(t_1) - C_{6:7,cp}(t_0)] + 4[C_{6:7,u}(t_1)V_u(t_1)]$  (Eq.11)

where  $V_p$  for an average size man is 3.0L and  $\beta = 1.1$

or

=  $4.4V_p [(2\beta) + 1] \times [C_{6:7,cp}(t_1) - C_{6:7,cp}(t_0)] + 4[C_{6:7,u}(t_1)V_u(t_1)]$  (Eq.12)

where  $V_p$  for an average size woman is 2.5L and  $\beta = 1.1$

#### 4. The $m_1$ demand ratio

At any point in time (t), the 1,25(OH) $D_3$ ,  $m_1$ , demand ratio ( $D_{r,i+e}$ ), expresses the ratio of the sum of end inactive metabolites of active vitamin D, 1,25(OH) $_2D_3$ ,  $m_1$  (i.e.  $m_8$ , +  $m_9$ , +  $m_{10}$ ) to the sum of non  $m_1$ , end inactive metabolites of 25(OH) $D_3$  (i.e.  $m_6$  +  $m_7$ ) in the intracellular plus extracellular compartments. The end inactive metabolites of 1,25(OH) $_2D_3$  track the portion of 25(OH) $D_3$  that goes on to make active vitamin D,  $m_1$ . The non  $m_1$  end inactive metabolites of 25(OH) $D_3$  track the portion of 25(OH) $D_3$  that is diverted away from making active vitamin D especially when the supply of active vitamin D is sufficient or in excess. See figures 2a&2b and expressions below. This ratio may reflect the body's demand for active vitamin D.

The total body nmoles of metabolite  $m_n$  at any time (t) in the intracellular and extracellular compartments is denoted:

$$M_{n,i+e}(t) \tag{D.2}$$

The quantity (nmoles) of active vitamin D, ( $m_1$ ), or  $M_1$  in the extracellular plus intracellular compartments at time (t) that has been synthesized can then be estimated using the assumed A.7 steady state synthesis pathways, [i.e.  $S_{0,1}(t) = S_{4,8}(t) + S_{5,9}(t) + S_{5,10}(t)$ ] and by using the assumptions A.4 and A.5 (i.e. the relationship between the mean intracellular compartment  $m_{8:10}$  concentrations and the extracellular compartment  $m_{8:10}$  concentrations):

$$C_{8:10,i}(t) = \beta C_{8:10,e}(t) = \beta C_{8:10,cp}(t) \quad (\text{A.5})$$

The nmoles of  $m_1$  in the intracellular plus extracellular compartments at time (t) can then be estimated to equal the nmoles of  $m_{8:10}$  in the intracellular plus the extracellular compartments:

$$M_{8:10}(t) = \beta C_{8:10,cp}(t)2V_e + C_{8:10,cp}(t)V_e \quad (\text{Eq.13})$$

Similarly, by using A.8 and substituting  $C_{6,7,cp}(t)$  into equation (13), the nmoles of  $m_0$  in the intracellular plus extracellular compartments diverted away from active vitamin D synthesis in nmoles can be estimated.

$$M_{6:7}(t) = \beta C_{6:7,cp}(t)2V_e + C_{6:7,cp}(t)V_e \quad (\text{Eq.14})$$

Equations 13 and 14 represent synthesized nmoles of  $m_{8:10}(t)$  and  $m_{6:7}(t)$  in the body excluding those metabolites excreted in urine or stool at time (t). See figures 2a and 2b.

Based on total intracellular and extracellular nmoles of end metabolites,  $m_{8:10}$  and  $m_{6:7}$  at time (t), the demand ratio of synthesized active vitamin D to vitamin D precursor diverted away from active vitamin D synthesis would be:

$$\text{Drm}_{1,i+e}(t) = \frac{M_{8:10,i+e}(t)}{M_{6:7,i+e}(t)} \quad (\text{Eq.15})$$

Note: When the nmoles of intracellular plus extracellular end inactive metabolites ( $m_{8:10}$ ) of active vitamin D, increase relative to the nmoles of the two end inactive metabolites ( $m_{6:7}$ ) of vitamin D precursor,  $m_0$ , the increase in  $\text{Drm}_{1,i+e}(t)$  may reflect up regulation of the production of  $1,25(\text{OH})_2\text{D}_3$  from  $25(\text{OH})\text{D}_3$  (i.e. up regulation of the C1 hydroxylase, CYP27B1 enzyme pathway and increased demand). When  $\text{Drm}_{1,i+e}(t)$  decreases the converse may be true. (Ref. 30, Figure 37.3) Again if the denominator becomes too small or cannot be measured, a factor of  $1 \times 10^{-9}$  can be added to the denominator to prevent the demand ratio from blowing up in size.

Similarly, based on total urine nmoles of end metabolites,  $m_{8:10}$  and  $m_{6:7}$ , the demand ratio of synthesized active vitamin D to vitamin D precursor diverted away from active vitamin D synthesis would be:

$$\text{Drm}_{1,u}(t) = \frac{M_{8:10,u}(t)}{M_{6:7,u}(t)} \quad (\text{Eq.16})$$

Both in the case of serum and urine, the reactions creating the end metabolites,  $m_{8:10}$  and  $m_{6:7}$  are assumed to be in a steady state condition. If the measurements of these end metabolites are made using the second assay with the CYP24A1 hydroxylase enzyme, the same mathematical expressions are used. However, the reactions creating the end metabolites,  $m_{8:10}$  and  $m_{6:7}$  would be driven to their end metabolites eliminating any intermediate metabolites by addition of the CYP24A1 hydroxylase enzyme. Again, the initial level of  $25(\text{OH})\text{D}_3$  in the serum

and urine must be measured and subtracted from the final  $m_{6:7}$  levels to get an accurate measurement of actual  $m_{6:7}$  in the plasma or urine.

### 5. The $m_0$ utilization percent

The  $m_0$  utilization percent at any one point in time (t) is defined as the ratio of the nmoles of  $m_{8:10,i+e}(t)$  divided by the nmoles of  $m_{8:10,i+e}(t)$  plus  $m_{6:7,i+e}(t)$  times 100%. Using the same derivations used in 4. above:

$$Ut\%m_{0,i+e}(t) = \frac{M_{8:10}(t)}{M_{8:10}(t) + M_{6:7}(t)} \times 100\% \quad (\text{Eq.17})$$

The 24 hour  $m_0$  utilization percent is defined as the ratio of the change in the nmoles of  $m_{8:10}(t_1, t_0)$  in the intracellular and extracellular compartments plus the accumulation of  $m_{8:10}(t_0, t_1)$  in the urine and stool over 24 hours divided by the sum of the total  $m_{8:10}(t_0, t_1)$  metabolites described above plus the change in the nmoles of  $m_{6:7}(t_1, t_0)$  in the intracellular and extracellular compartments plus the accumulation of  $m_{6:7}(t_0, t_1)$  nmoles in the urine and stool over 24 hours.

$$\begin{aligned}
 \int_{t_0}^{t_1} U' t\% m_0 dt = & \frac{\int_{t_0}^{t_1} S_{0,1}(t) dt}{\int_{t_0}^{t_1} S_{0,1}(t) dt + \int_{t_0}^{t_1} S_{0,2:3}(t) dt} \times 100\% \quad (\text{Eq.18}) \\
 & \text{male female} \\
 & \text{Eq.9/M or 10/F} \\
 & \text{Eq.9/M or 10/F + Eq.11/M or 12/F}
 \end{aligned}$$

## 6. Percent Increase or Decrease of the above Parameters over Time

Percent Increase or decrease of the parameters above including estimates of synthesis of active vitamin D over 24 hours, active vitamin D demand ratios, 25(OH)D<sub>3</sub> percent utilization, and biomarkers for total active vitamin D synthesis at any time t, over the time interval t<sub>n+1</sub> and t<sub>n</sub> can be determined by taking the ratio of a parameter at time t<sub>n+1</sub> divided by the same parameter at time t<sub>n</sub>, minus 1, and then times 100%. For example:

$$\frac{[\text{Drm}_{1,i+e}(t_{n+1})] - [\text{Drm}_{1,i+e}(t_n)]}{[\text{Drm}_{1,i+e}(t_n)]} \times 100\% \quad (\text{Eq.19})$$

Note: As long as the same technology to determine the above parameters is used by different labs, and as long as the measurements which are made at different labs have consistent measurement technique variations between sequential runs, the ratios or percent change should be largely independent of the particular labs technique variations from other labs.

## References

1. Panagiotou G, Tee SA, Ihsan Y, Athar W, Marchitelli G, Kelly D, Boot CS, Stock N, Macfarlane J, Martineau AR et al. Low serum 25-hydroxyvitamin D, 25(OH)D, levels in patients hospitalized with COVID-19 are associated with greater disease severity. *Clinical Endocrinology - Letter*, 03 July 2020. doi:10.1111/cen.14276 assessed 14 July 2020 at <https://onlinelibrary.wiley.com/doi/abs/10.1111/cen.14276>
2. Carpagnano GE, Di Lecce V, Quaranta VN, Zito A, Buonamico E, Capozza E, Palumbo A, Di Giola, Valerio VN, and Resta O. Vitamin D deficiency as a predictor of poor prognosis in patients with acute respiratory failure due to COVID-19. *Journal of Endocrinological Investigation* 09 Aug 2020; [www//doi.org/10.1007/s40618-020-01370-x](http://www.doi.org/10.1007/s40618-020-01370-x)
3. Goddek, S. Vitamin D3 and K2 and their potential contribution to reducing the COVID-19 mortality rate. *International Journal of Infectious Diseases* 2020; 99: 286-290
4. Castillo ME, Costa LME, Barrios JMV, Diaz JFA, Miranda JL, Bouillon R, and Gomez JMQ. Effect of calcifediol treatment and best available therapy verses best available therapy on intensive care unit admission and morality among patients hospitalized for COVID-19: A pilot randomized clinical study. *Journal of Steroid Biochemistry and Molecular Biology* 203 (29 Aug. 2020) 105751
5. Ye K, Tang F, Liao X, Shaw BA, Deng M, et al. Does serum Vitamin D level Affect COVID-19 Infection and its Severity? – A Case-Control Study. *Journal of the American College of Nutrition*, 13 Oct. 2020; DOI: [10.1080/07315724.2020.1826005](https://doi.org/10.1080/07315724.2020.1826005)
6. Meltzer DO, Best TJ, Zhang H, Vokes T, Arora V, Solway J. Association of Vitamin D Status and Other Clinical Characteristics with COVID 19 Test Results. *JAMA Network Open*. 2020; 3(9): 1-12 e2019722
7. Grant WB, Lahore H, McDonnell SL, Baggerly CA, French CB, Aliano JL, and Bhattoa HP. Evidence that Vitamin D Supplementation Could Reduce Risk of Influenza and COVID-19 Infections and Deaths. *Nutrients* 2020, 12, 988 pgs. 1-19
8. Lanham-New SA, Webb AR, Cashman KD, et al. Vitamin D and SARS-Co V-2 virus/COVID-19 Disease. *BMJ Nutrition, Prevention and Health* 2020;0. Doi:10.1136/bmjnph-2020-000089.
9. Adams JS, Hewison M: Unexpected actions of vitamin D - new perspective on the regulation of innate and adaptive immunity. *Nat Clin Pract Endocrinol Metab*. 2008 February; 4(2): pp.1-17
10. Hewison M: Vitamin D and the intracrinology of innate immunity. *Mol Cell Endocrinol*. 2010 June 10; 321(2): pp. 103-111  
*Endocrinol*. 2010 June 10; 321(2): pp. 103-111

11. Charoenngam N, Holick MF. Immunologic Effects of Vitamin D on Human Health and Disease - Review. *Nutrients* 2020, 12, 2097
12. InformedHealth.org [Internet] . Cologne, Germany: Institute for Quality and Efficiency in Health Care (IQWiG) ; 2006 - . What are the organs of the immune system? [Updated 2020 Jul 30]. Available from: <https://www.ncbi.nlm.nih.gov/books/NBK279395/>
13. Biesalski HK. Vitamin D deficiency and co-morbidities in COVID-19 patients- A fatal relationship? *Nfs Journal* 2020 Aug; 20: 10-21
14. Lindo A, Lushington GH, Abello J, Melgarejo T. Clinical Relevance of Cathelicidin in Infectious Disease. *J Clin Cell Immunol* 2013. S13; 003: 1-11
15. Youssef DA, Miller CWT, El-Abbassi AM, Cutchins DC, Cutchins C, Grant WB, and Peiris AN. Antimicrobial implications of vitamin D. *Dermato-Endocrinology* 2011. 3;4: 220-229
16. Sassi F, Tamone C, D'Amelio P. Vitamin D: Nutrient, Hormone, and Immunomodulator. *Nutrients* 2018, 10, 1656; doi:10.3390/ nu10111656
17. Calton EK, Keane KN, Newsholme P, and Soares MJ: The Impact of Vitamin D Levels on Inflammatory Status: A Systematic Review of Immune Cell Studies. *PLOS ONE* 03 Nov. 2015; 10(11): 1-12, e0141770
18. Speddings S, Vanlint S, Morris H, and Scraggs R. Does Vitamin D Sufficiency Equate to a Single Serum 25-Hydroxy Vitamin D level or Are Different Levels Required for Non Skeletal Diseases? *Nutrients* 2013, 5, 5127-5139
19. Schoenmakers I, and Jones KS. Metabolism and Determinants of Metabolic Fate of Vitamin D, pg. 642, Chapt. 37: Pharmacology and Pharmacokinetics, In *Vitamin D 4<sup>th</sup> Edition, Vol. 1 Biochemistry, Physiology, and Diagnostics*. Editors: Feldman D, Pike JW, Bouillon R, Giovannucci E, Goltzman D, and Hewison M. Academic Press, Elsevier Inc., San Diego, 2018
20. Need AG, O'Loughlin PD, Morris HA, Coates PS, Horowitz M, and Nordin BEC. Vitamin D metabolites and calcium absorption in severe vitamin D deficiency. *J Bone Miner Res* 2008, 23: 1859-63
21. Jones G, Prosser D, Kaufmann M. Thematic Review Series: Fat-Soluble Vitamins: Vitamin D, Cytochrome P450-mediated metabolism of vitamin D. *Journal of Lipid Research* 2014; Vol. 55: 13-31
22. Tamblyn JA, Jenkinson C, Larner DP, Hewison M, and Kilby MD. Serum and Urine vitamin D metabolite analysis in early preeclampsia. *Endocrine Connections* (2018); 7, 199-210
23. Fairbrother B, Shippee RL, Kramer T, Askew W, Mays M, Popp K, Kramer M, Hoyt R, Tulley R, Rood J, Delany J, Frykman P, Marchitelli L, Arsenault J, Tessicini M, and Jezior D. Nutritional and Immunological Assessment of Soldiers During the Special Forces Assessment and Selection Course. Technical Report T95-22 U.S. Army Research Institute of Environmental Medicine, Natick, Massachusetts, September 1995  
<https://apps.dtic.mil/dtic/tr/fulltext/u2/a299556.pdf> Assessed Jan 19, 2019

24. Jones KS, Redmond J, Fulford AJ, Jarjou L, Zhou B, Prentice A, and Schoenmakers I. Diurnal rhythms of vitamin D binding protein and total and free vitamin D metabolites. *J Steroid Biochem Mol Biol.* 2017;172:130-5
25. French CB, McDonnell SL, and Reinhold V. 25-Hydroxyvitamin D variability within-person due to diurnal rhythm and illness: a case report. *Journal of Medical Case Reports* 2019;13:29
26. Jolliffe DA, Walton RT, Griffin CJ, and Martinean AR. Single nucleotide polymorphism in the vitamin D pathway associating with circulating concentrations of vitamin D metabolites and non-skeletal outcomes-Review of genetic association studies. *J. Steroid Biochem Mol Biol*-2016 Nov; 164: 18-29
27. St-Arnaud R and Jones G. CYP24A1: Structure, Function, and Physiological Role. Ch. 6, 82-84. *Pharmacology and Pharmacokinetics, In Vitamin D 4<sup>th</sup> Edition, Vol. 1 Biochemistry, Physiology, and Diagnostics.* Editors: Feldman D, Pike JW, Bouillon R, Giovannucci E, Goltzman D, and Hewison M. Academic Press, Elsevier Inc., San Diego, 2018
28. Fagerberg L, Hallstrom BM, Oksvoldt P, Kamp C, Djureinovic D, Odeberg J, et al. Analysis of the Human Tissue-Specific Expression by Genome-wide Integration of Transcriptions and Antibody based Proteomics. *Molecular and Cellular Proteomics* 2014 13:10; 397-406
29. PKM-Array Suite, WIKI, Report Gene Transcript Counts.  
<http://www.arrayserver.com/wiki/index-php?title=RPKM> Assessed 17 April 2019
30. CYP27A1 cytochrome P450 family 27 subfamily A member 1 [Homo sapiens (human)] HPA RNA- seq. normal tissues, Bio Project PRJEB 4337, PMID 24309898  
<https://www.ncbi.nlm.nih.gov/gene/1593> Accessed 15 April 2019
31. CYP2R1 cytochrome P450 family 2 subfamily R member 1 [Homo sapiens (human)] HPA RNA- seq. normal tissues, Bio Project PRJEB 4337, PMID 24309898  
<https://www.ncbi.nlm.nih.gov/gene/120227> Accessed 15 April 2019
32. CYP3A4 cytochrome P450 family 3 subfamily A member 4 [Homo sapiens (human)], HPA RNA- seq. normal tissues, Bio Project PRJEB 4337, PMID 24309898  
<https://www.ncbi.nlm.nih.gov/gene/1576> Accessed 15 April 2019
33. CYP27B1 cytochrome P450 family 27 subfamily B member 1 [Homo sapiens (human)], HPA RNA- seq. normal tissues, Bio Project PRJEB 4337, PMID 24309898  
<https://www.ncbi.nlm.nih.gov/gene/1594> Accessed 15 April 2019
34. CYP24A1 cytochrome P450 family 24 subfamily A member 1 [Homo sapiens (human)], HPA RNA- seq. normal tissues, Bio Project PRJEB 4337, PMID 24309898  
<https://www.ncbi.nlm.nih.gov/gene/1591> Accessed 15 April 2019

35. Ciprini C, Pepe J, Piemonte S, Colangelo L, Cilli M and Minisola S. Review Article: Vitamin D and Its Relationship with Obesity and Muscle. *International Journal of Endocrinology*, Vol. 2014, pg. 1-11
36. Ceglia L. Vitamin D and its role in skeletal muscle. *Current Opinion in Clinical Nutrition and Metabolic Care* 2009. Vol. 12, No. 6, pp. 628-633
37. Cirgia CM, Clifton-Bligh RJ, Mokbel N, Cheng K, and Gunton JE. Vitamin D signaling regulates proliferation, differentiation, and myotube size in C<sub>2</sub>C<sub>12</sub> skeletal muscle cells. *Endocrinology* 2014: Vol. 155; No. 2, pp. 347-357
38. Molner F, Siqueiro R, Sato Y, Araujo C, Schuster I, Antony P, Peluso J, Muller C, Mourino A, Moras D, and Rochel N. 1 $\alpha$ ,25(OH)<sub>2</sub>-3-Epi-Vitamin D<sub>3</sub>, a Natural Physiological Metabolite of Vitamin D<sub>3</sub>: Its Synthesis, Biological Activity and Crystal Structure with Its Receptor. *PLoS ONE* March 2011: Volume 6: Issue 3, 1-11. e18124
39. Schoenmakers I, and Jones KS. Muscle and Adipose Tissue, pg. 640, and Body Pool of Vitamin D and 25(OH)D, Ch. 37, 641: Pharmacology and Pharmacokinetics, In *Vitamin D 4<sup>th</sup> Edition*, Vol. 1 Biochemistry, Physiology, and Diagnostics. Editors: Feldman D, Pike JW, Bouillon R, Giovannucci E, Goltzman D, and Hewison M. Academic Press, Elsevier Inc., San Diego, 2018
40. Heaney RP, Horst RL, Cullen DM, and Armas LAG. Vitamin D<sub>3</sub> distribution and status in the body. *J Am Coll. Nutr* 2009; 28: 252-6
41. Avioli LV, Lee SW, McDonald JL, and DeLuca HF. Metabolism of Vitamin D<sub>3</sub> – <sup>3</sup>H in Human Subjects: Distribution in Blood, Bile, Feces, and Urine. *Journal of Clinical Investigation* 1967. Vol.46: No.6; 983-992
42. Gray RW, Caldas AE, Wilz DR, Lemann J Jr., Smith GA, and DeLuca HF. Metabolism and excretion of <sup>3</sup>H – 1,25(OH)<sub>2</sub> vitamin D<sub>3</sub> in Healthy Adults. *J Clin Endocrinol Metabolism* 1978 May; 46(5): 756-65
43. Kumar SR, Hunder GG, Heath III SH, Riggs BL. Production, Degradation, and Circulating Levels of 1,25- Dihydroxyvitamin D in Health and in Chronic Glucocorticoid Excess. *J. Clinical Investigation* October 1980: Vol. 66: 664-669
44. Physiology Figure: Body Fluid Compartments of a 55-Kg Adult Woman. PhysiologyWeb [https://www.physiologyweb.com/figures/physiology\\_figure\\_br8Yb3P5GjRwXw49PleVuplynmn77aw4\\_body\\_fluid\\_compartments\\_of\\_a\\_55\\_kg\\_adult\\_woman.html](https://www.physiologyweb.com/figures/physiology_figure_br8Yb3P5GjRwXw49PleVuplynmn77aw4_body_fluid_compartments_of_a_55_kg_adult_woman.html) Assessed 8/12/2019
45. Physiology Figure: Body Fluid Compartments of a 70-Kg Adult Man. PhysiologyWeb [https://www.physiologyweb.com/figures/physiology\\_illustration\\_tPksfgTyDcZ10zEq1Wp1FqLjrBRL8IGL\\_body\\_fluid\\_compartments\\_of\\_a\\_70\\_kg\\_adult\\_man.html](https://www.physiologyweb.com/figures/physiology_illustration_tPksfgTyDcZ10zEq1Wp1FqLjrBRL8IGL_body_fluid_compartments_of_a_70_kg_adult_man.html)
46. Vitamin D-dependent rickets, Genetics Home Reference, U.S. National Library of Medicine, NIH. <https://ghr.nlm.nih.gov/condition/vitamin-d-dependent-rickets#genes> assessed on 18 June 2020

47. Pasquali M, Tartaglione, Rotondi S, Muci ML, Mandanici G, Farcomeni A, Marangella M, and Mazzaferro S. Calcitriol/calcifediol ratio: Indicator of vitamin D hydroxylation efficiency? *BBA Clinical* 3 (2015) 251-256
48. Schoenmakers I, and Jones KS. Muscle and Adipose Tissue, pg. 640, and Metabolism add Determinants of Metabolic Fate of Vitamin D, Figure 37.3, Overview of metabolic pathways with different ranges of vitamin D status, Ch. 37, 641: Pharmacology and Pharmakinetics, In *Vitamin D 4<sup>th</sup> Edition*, Vol. 1 Biochemistry, Physiology, and Diagnostics. Editors: Feldman D, Pike JW, Bouillon R, Giovannucci E, Goltzman D, and Hewison M. Academic Press, Elsevier Inc., San Diego, 2018
49. Zelser S, Goessler W, and Herrmann M. Measurement of vitamin D metabolites by mass spectrometry, and analytical challenge. *J. of Lab and Precis Med* 2018; 3:99
50. Muller MJ, Volmer DA. Mass Spectrometric Profiling of Vitamin D Metabolites beyond 25-Hydroxyvitamin D. *Clinical Chemistry* 2015 Aug; 61:8, 1033-1048
51. Abu Kassim NS, Shaw PN, and Hewavitharana AK. Simultaneous determination of 12 vitamin D compounds in human serum using online sample preparation and liquid chromatography-tandem mass spectrometry. *Journal of Chromatography A*; 19 January 2018. Volume 1533: pgs. 57-65
52. Nur Sofiah Abu Kassim. Development of an assay for vitamin D in biological samples; Ch. 2, PhD. Thesis, University of Queensland, Australia, 2017 Assessed May 15, 2020 at; <https://espace.library.uq.edu.au/view/UQ:728352>
53. Calcitroic Acid, Calcioic Acid. Toronto Research Chemicals. 20 Martin Ross Ave, North York, ON M3J 2K8, Canada 1-416-665-9696, (USA and Canada 1-800-727-9240) Assessed Oct 30, 2020 at <https://www.trc-canada.com/products-listing/>
54. CYP24A1 (Human) Recombinant Protein, Biocompare.Com. Accessed 7/17/2020 at <https://biocompare.com/Search-Biomolecules/?search=CYP24A1>
55. Sakaki T, Sawada N, Nonaka Y, Ohyama Y, and Inouye K. Metabolic studies using recombinant Escherichia coli cells producing rat mitochondrial CYP24 – CYP24 can convert 1 $\alpha$ ,25-dihydroxyvitamin D<sub>3</sub> to calcitroic acid. *Eur. J. Biochem.* 262,43-48 (1999)
56. McGonagle D, Sharif K, O'Regan A, and Bridgewood C. The Role of Cytokines including Interleukin-6 in COVID-19 induced Pneumonia and Macrophage Syndrome-Like Disease. *Autoimmunity Rev.* 2020 Jun; 19(6):102537
57. Hydroxyvitamin D Calculator for Seasonal Adjustment, Kidney Research Institute, University of Washington. Available at <https://kri.washington.edu/calculator> assessed 31 January 2019
58. Sachs MC, Shoben A, Levin GP, Robinson-Cohen C, Hoofnagle AN, Swords-Jenny N, et al: Estimating mean annual 25-hydroxyvitamin D concentrations from single measurements: the Multi-Ethnic Study of Atherosclerosis. *Am J Clin Nutr* 2013; 97: 1243-51

59. Vitamin D Calculator. GrassrootsHealth Nutrient Research Institute. Assessed July 31, 2020 at [www.grassrootshealth.net/project/dcalculator/](http://www.grassrootshealth.net/project/dcalculator/)
60. Heaney RP, Armas L AG, Shary JR, Bell NH, Binkley N, and Hollis BW. 25-Hydroxylation of vitamin D<sub>3</sub>: relation to circulating vitamin D<sub>3</sub> under various input conditions. *Am J Clin Nutr* 2008;87:1738-42.
61. Groningen LV, Opdenoordt S, Sorge AV, Telting D, Giesen A, and Boer HD. Cholecalciferol loading dose guideline for vitamin D-deficient adults. *European Journal of Endocrinology* (2010); 162: 805-811
62. Vieth R. Vitamin D supplementation, 25-hydroxyvitamin D concentrations, and safety. *Am J Clin Nutr* 1999; 69: 842-56
63. Kaufman HW, Niles JK, Kroll MH, Bi C, Holick MF. SARS-CoV-2 positivity rates associated with circulating 25-hydroxyvitamin D levels. *PLOS ONE* 17 Sept. 2020: 15(9); e0239252. <https://doi.org/10.1371/journal.pone.0239252> Assessed on 27 Sept. 2020

**Funding:** Salisbury Foundation for Research and Education, National Association of Veterans' Research and Education Foundations, NAVREF

**Declaration of Interest:** The authors declare that they have no known competing financial interests or personal relationships that could have appeared to influence the work reported in this paper.

**Consent statement/Ethical approval:** Not required.

**Acknowledgements:** This paper is based in part upon research supported by the U.S. Department of Veterans Affairs, Research Department, W.G. (Bill) Hefner VA Medical Center, Salisbury, NC. The welfare of human subjects was protected and the W.G. (Bill) Hefner VA Medical Center Institutional Review Board and Research Committee approved all research involving human subjects. (Study: IRB Protocol 18-020 – “Medical Evaluation of U.S. Veterans with Chronic Multi-symptom illnesses”).

Sean R Maloney is a part-time physician employee of the U.S. Government. This work was prepared as part of his official duties. Title 17, USC, 105 provides that “Copyright protection under this title is not available for any work of the U.S. Government”. Title 17, USC, 101 defines a U.S. Government work as “a work prepared by an employee of the U.S. Government as part of that person’s official duties”.

Matthew Maloney Ph.D., is a quantitative modeling consultant residing in Ft. Collins, CO.

## **Author Contributions:**

Sean R Maloney M.D.: Conceptualization, writing of paper, and creation of Mathematical Model and Figures 1, and 2a-2d.

Matthew H Maloney Ph.D.: Conceptualization and writing of paper, creation of Mathematical Model and assumptions.

**Disclaimer:** The views expressed in this paper are solely those of the authors and do not reflect those of the Department of Veterans Affairs or the City of Hope Comprehensive Cancer Center.

## **Other Contributors:**

The following individuals have kindly reviewed this manuscript and added timely and helpful comments improving the content of this paper:

Maria E. Ariza, Ph.D.\*

Marshall Williams, Ph.D.\*

Paula Goolkasian, Ph.D.\*\*

Amitha K. Hewavitharana\*\*\*

\*Department of Cancer, Biology, and Genetics

Institute for Behavioral Medicine Research

The Ohio State University

460 Medical Center Dr., Columbus, Ohio 43210

\*\*Dept. of Psychological Science

University of North Carolina at Charlotte

9201 University City Blvd., Charlotte, NC 28223

\*\*\*School of Pharmacy

University of Queensland

QLD 4072, Australia